

Acoustic Condition Assessment of Concrete Sewer Pipes using a Particle Velocity Sensor

A.A. (Adriaan) Pleijsier

MSc Report

Committee:

Dr.ir. D. Dresscher
H. Noshahri, MSc
Prof.dr.ir. G.J.M. Krijnen
Dr.ir. L.L. Olde Scholtenhuis

April 2019

012RAM2019
Robotics and Mechatronics
EE-Math-CS
University of Twente
P.O. Box 217
7500 AE Enschede
The Netherlands

Summary

In this report it is researched to what extent an acoustic impact echo using a particle velocity sensor can assess the condition of a concrete sewer pipe. Multiple sub-questions have been answered using both literature and experiments.

The failure process of a collapsing concrete sewer pipe is studied. Three aspects are interesting for condition assessment: The sewer wall thickness, lack of supporting material and missing pieces of concrete. All three situations are converted to experiments with flat concrete tiles as samples.

The wall thickness should be easy measurable by looking at the thickness frequency. The lack of support material is harder to detect especially when the supporting soil is dry. Missing concrete pieces - flaws - are detectable depending on the size-depth ratio. If the flaw is small or far under the surface it becomes harder to detect.

The contact time of the impactor determines which frequencies are excited in the concrete. If the impact is shorter, the vibrations will contain more high frequencies. It is important that the excited frequencies are higher than the frequencies interesting for analysis, which is in most cases the thickness frequency.

The particle velocity sensor should be placed in the very near field in order to benefit for the background noise reduction compared to a microphone. The response of the sensor can be linearized up to 20 kHz when the provided correction filter is used, gain and phase for higher frequencies are not specified.

The developed impact device has a too long contact time, which is seen in all results by the damping of interesting frequency peaks. Nevertheless, some local frequency peaks could be linked to expected frequency peaks. For unknown samples the condition cannot be assessed.

Measuring in humid sewer conditions should not be a problem. Concrete soaked with water shows an identical response as dry concrete. However, a layer of water on the surface should be avoided because this suppresses all surface vibrations.

The background noise cancellation of the particle velocity sensor is measured. As expected, only low frequencies are measured in the very near field. Interesting high frequencies are influenced by the background noise, therefore the advantage over microphone disappears. A microphone seems like a more suitable sensor due to its higher sensitivity for higher frequencies.

To conclude, the use of a particle velocity sensor for impact echoes is not advised. Experiments indicate that the microphone has an increased sensitivity for higher frequencies and is still usable with background noise. Therefore - although the particle velocity sensor is useable - a microphone is probably a better measurement tool for assessing the condition of concrete sewer pipes contactless than the particle velocity sensor.

The main recommendation is to do comparative measurements with a traditional impact echo using a surface mounted transducer. This way it can be verified if the experiments are executed correctly and can the particle velocity sensor performance be evaluated correctly.

Preface

The process of writing this master thesis was an adventure. I looked up to writing my thesis even before starting my master. The research side of the university never interested me much. Once started this all faded.

At the beginning of this project I did not think the research would have ended in by listening to tiles with a particle velocity sensor. From a first prototype, to laser measurements, destructive test in the civil engineering lab to using my band's sound gear: although not all mentioned in this report, it all helped to get to this point.

I would like to thank Hengameh Noshahri and Douwe Dresscher for their daily supervision. Without their enthusiasm, encouragement, discussion and feedback I would never have finished this report.

Adriaan Pleijsier
Enschede, 9 April 2019

Contents

List of symbols	1
1 Introduction	2
1.1 Context	2
1.2 Goal	3
1.3 Outline	3
2 Background	4
2.1 Introduction to impact echoes	4
2.2 Very near field	5
3 Analysis	8
3.1 Sewer condition determining aspects	8
3.2 Condition influences on vibrations resulting from impact	9
3.3 Vibrations in concrete induced by impactor	11
3.4 Measuring vibrations contactless with particle velocity sensor	12
4 Experimental setup	15
4.1 Sewer setup	15
4.2 Impact device	17
4.3 Particle velocity sensor	19
4.4 Signal processing	20
4.5 Total setup	21
5 Experiments	23
5.1 Validation of setup	24
5.2 Varying thickness	25
5.3 Varying cavity support	28
5.4 Varying cavity concrete	30
5.5 Varying background noise	33
5.6 Varying surface humidity	37
6 Conclusion & Recommendations	40
6.1 Conclusion	40
6.2 Recommendations	40
A Sand composition	42
B Impact device wiring details	43

B.1 User I/O	43
B.2 Solenoid	44
B.3 Sensors and micro-controller	45
C Impact device Arduino code	47
Bibliography	50

List of symbols

Symbol	Unit	Meaning
β	[-]	Correction factor for the P-wave speed
C	[m/s]	Wave speed
d	[m]	Lateral dimension of reflecting interface
D	[m]	Diameter
E	[Nm ⁻²]	Young's modulus
E_{kin}	[J]	Kinetic energy
F	[N]	Force
f	[Hz]	Frequency
f_T	[Hz]	Thickness frequency
λ	[m]	Wavelength
L	[m]	Length or typical sound source size
m	[kg]	Mass
ρ	[kgm ⁻³]	Density
R_{coef}	[-]	Reflection coefficient
r_n	[m]	Normal distance to sound source
SNR	[-]	Signal-to-Noise Ratio, can be displayed in [dB]
T	[m]	Plate thickness or flaw depth
t	[s]	Time
t_c	[s]	Contact time
U	[V]	Voltage
ν	[-]	Poisson's ratio
v	[m/s]	Speed
W	[m]	Width
Z	[Pasm ⁻³]	Acoustic impedance

1 Introduction

1.1 Context

All around the world, important infrastructures are buried underground. Fresh water, gas, sewer pipes, electric power, communication networks: most of them are out of sight. The location and condition of these underground infrastructures are mostly unknown, therefore it is a challenge to maintain these infrastructures. Condition assessment of sewer pipes is part of the TISCALI (Technology Innovation for Sewer Condition Assessment - Long-distance Information-system) project (Prof. dr. Z. Su, 2017). The Water Resources department, department of Construction Management and Engineering, and Robotics and Mechatronics department are involved in this project.

Sewer pipes are mostly made of reinforced concrete. The diameter of these pipes varies from centimetres to man-sized pipes. Due to the hazardous environment most inspections are done remotely. An example robot is displayed in figure 1.1. During inspection the sewer is only inspected visually. Flaws seen on the sewer surface can be detected, but cavities and internal flaws are unnoticed by camera inspections.



Figure 1.1: Current available sewer inspection robot of ID-tec (<https://www.id-tec.nl/>)

Non-destructive technologies are developed to determine the structural integrity (under the surface) of concrete without damaging it. With these non-destructive techniques cavities, internal flaws and even strength properties can be determined. Multiple non-destructive methods are available, for example Schmidt rebound hammer, Ultra Velocity Pulses, Impact Echoes and more. Nevertheless, none of these are directly suitable for in-situ use in sewers (Helal et al., 2015).

When used appropriately, impact echoes can give a good estimation of the invisible condition of concrete (Carino, 2015). In this method, a steel ball generates an impact on surfaces. A vibration analysis can be performed by mounting a transducer on the same side as where the impact is generated. The drawback of this method is that the transducer needs to be mounted on the sewer surface. When not mounted precisely, none or faulty data is collected. When this requirement can be overcome, the impact echo technique could be useful.

Impact echoes can also be done acoustically using a microphone as sensor (Zhu and Popovics, 2007). The transducer on the surface is replaced with a microphone aimed at the surface. In this way no contact with the surface is required, except for impact generation. The induced surface vibrations cause air particles to be excited, which then can be measured with a microphone. A drawback of this method is the influence of background noise on the measurements. This noise is caused by echoes of the impact itself and contaminates the signal obtained from the surface vibrations. A particle velocity sensor could be a solution for this problem, because it can measure excited air particles near the surface with less influence of background noise.

1.2 Goal

There is no research available about the use of a particle velocity sensor in impact echoes, let alone the combination with sewer condition assessment. Therefore the goal of this work will be to investigate the possibilities of using the particle velocity sensor in combination with the impact echo technique to determine the condition of sewer pipes.

The main research question is stated: *To what extent can an acoustic impact echo using a particle velocity sensor assess the condition of a concrete sewer pipe?* This is further split in sub-questions.

1. What determines the condition of a concrete sewer pipe?
This question is answered by literature. The experiment design is based on this study.
2. How do surface vibrations resulting from an impact reflect the material condition?
Vibration characteristics are linked to material properties by literature. With this theory expected results of the experiments are predicted.
3. What impact is required for a successful measurement?
Factors influencing the vibrations generated by the impact in the concrete are discussed. These factors are linked to the impact echo requirements.
4. How to measure these surface vibrations contactless using a particle velocity sensor?
The surface vibrations are measured acoustically using a particle velocity sensor. The working principle of the particle velocity sensor and why background noise should have less influence is discussed.

1.3 Outline

After an introduction, background information for readers unfamiliar with impact echo technology and the very near field is found in chapter 2. A thorough analysis is done in chapter 3. The structure of the analysis chapter is similar to the research questions. The answers of the analysis are tested with means of experiments. The experimental setup is discussed in chapter 4 and the experiments with results in chapter 5. With the analysis knowledge a hypothesis for each experiment is made. The actual results are shown, discussed and compared with the expected results. In the conclusion - chapter 6 - the final answers to the research questions are shown, as well as recommendations for further research.

2 Background

2.1 Introduction to impact echoes

This chapter is meant for readers unfamiliar with impact echo technology. The most important parts of this technology required for this research are discussed and explained.

The basic principle of an impact echo is shown in figure 2.1. The displacement after an impact is measured by a transducer on the surface. A Fourier transform shows the frequency content of this signal. Some frequency peaks can be correlated to the internal material composition.

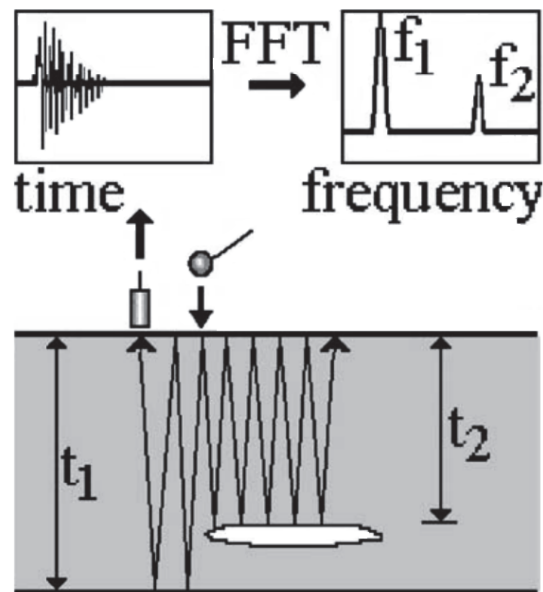


Figure 2.1: Impact echo principle (Colla and Lausch, 2003)

2.1.1 Waves in concrete

The impact induces vibrations in the concrete. Three types of vibrations are observed in the material: Pressure (P), Shear (S) and Rayleigh (R) waves. The three different waves all have different particle motion. In the P-waves particles have motion parallel to the propagation direction. S-waves have particle motion perpendicular to the propagation direction. R-waves travel only near the surface, the particles move in a retrograde elliptical way. The speed of these waves varies (see figure 2.2) and depends on material properties.

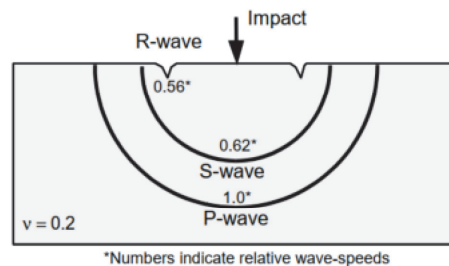


Figure 2.2: Different types of waves (Carino, 2001)

Because the R-wave only travels through the surface layer, it does not contain information about the underlying material. The S-wave particle motion is perpendicular to the wave mo-

tion. Therefore results the reflection of the S-wave on the back of the material in a left-to-right motion on the surface. These do not result in measurable vibrations like the P-wave. Only the P-wave reflections contains clear data about the underlying material. Therefore only P-waves are important for impact echo assessment.

The P-wave travels the fastest, but has the lowest energy content (Carino, 2015). Its speed is calculated by:

$$C_p = \sqrt{\frac{E(1-\nu)}{\rho(1+\nu)(1-2\nu)}} \quad (2.1)$$

Where C_p is the pressure wave speed, E the Young's modulus of elasticity, ν the Poisson's ratio and ρ the density. For concrete the P-wave speed is expected to be between 2000 ms^{-1} and 4000 ms^{-1} .

2.1.2 Reflections

The P-wave reflects on parts with a different specific acoustic impedance (Z), such as material boundaries. The amount of reflection (R_{coef}) is determined by the angle of incidence and the difference between the materials. For a normal incidence (90°) the reflection coefficient is the highest and given by:

$$R_{coef} = \frac{Z_2 - Z_1}{Z_2 + Z_1} \quad (2.2)$$

The wave travels from material 1 to 2. Z_1 is the specific acoustic impedance of material 1 and Z_2 of material 2. The reflections can be measured on the surface. When the reflection is negative, the wave changes from compression to decompression or vice versa. By analysing all reflections, the thickness of the concrete can be estimated as well as internal flaws.

The thickness can be estimated using the thickness frequency f_T . This is the frequency which depends on the total thickness of the concrete. The impact needs to include the thickness frequency, otherwise the thickness cannot be determined (Carino, 2015). It is calculated by:

$$f_T = \frac{\beta C_p}{2T} \quad (2.3)$$

Where β is correction factor (explained next), C_p is the P-wave speed and T the plate thickness. Traditionally the β correction factor is set empirically to 0.96 for plate structures. Further research of Gibson and Popovics (2005) gives β physical meaning (Zero-Group-Velocity S_1 Lamb mode, which is out of the scope of this research) and correlates it to the Poisson ratio.

2.1.3 Analysis

In figure 2.3 a typical displacement waveform after impact is shown. The R-wave (which travels the slowest) is measured first and has a high displacement compared to the P-wave. This is because it does not need to reflect in order to be measured. The R-wave should be ignored to avoid disturbance of the P-wave analysis.

After removal of the R-wave, the signal should be analysed in the frequency domain. In the frequency domain, certain peaks can be linked to material characteristics. When the P-wave speed is known, the thickness frequency peak (f_T) is used to calculate the material thickness. Other peaks can indicate flaw and cavities in the concrete.

2.2 Very near field

In any sound field the sound pressure p and particle velocity u are related by the specific acoustic impedance Z (de Bree et al. (2004)). In the far field - beginning two wavelengths from the source - the sound pressure and particle velocity are in phase and at equal level. Near the source of the sound, the straightforward far field properties vanish and the very near field comes into

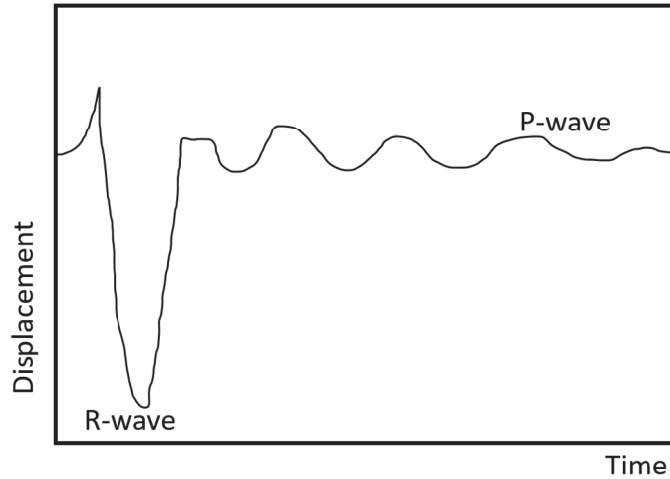


Figure 2.3: Typical displacement waveform

the picture. There are two conditions applicable to the very near field:

$$r_n \ll \frac{L}{2\pi} \ll \frac{\lambda}{2\pi} \quad (2.4)$$

r_n is the normal distance to the sound source, L is the typical source size and λ is the wavelength. In figure 2.4 the parameters are displayed. This means:

- The measurement distance should be closer than the size of the vibrating object divided by 2π .
- The wavelength of the sound should be larger than the size of the vibrating object. This condition is a limitation of the measurable frequencies in the very near field when the sound source size is constant.

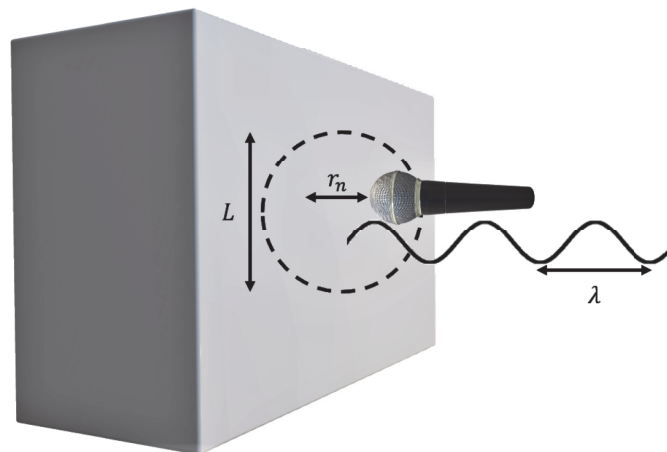


Figure 2.4: Parameters for very near field condition. The dashed circle indicates the vibrating surface.

Particles can be seen as incompressible fluid in the very near field. Sound pressure is the compression and decompression of air, which is suppressed. Therefore the sound pressure level is low compared to the particle velocity level in the very near field. The influence of the distance to the sound source is little in the very near field.

Sound waves belonging to background noise reflect on rigid surfaces. These reflections can cause the pressure to double when it is near a surface. The particle velocity sensor will not

measure the background noise wave, due to the fact that the particles of the wave and its reflection move in opposite directions (de Bree and Druyvesteyn, 2005).

Due to the strong received vibration signal of a surface when in the very near field and the reduced influence of the background noise, particle velocity measurements are an interesting option for contactless surface vibration measurement in a noisy environment (Comesana et al., 2014).

3 Analysis

The research questions are answered by means of a literature study. This research only focuses on non-visible or hardly visible condition assessment.

3.1 Sewer condition determining aspects

When assessing the condition of concrete sewer pipes, it is important to know what aspects of the pipe determine its condition. In this section we first look at the time-line of sewer failures, then the failure process. At last the measurable condition aspects are discussed.

3.1.1 Failure time-line

By looking at the failure probability over time (see figure 3.1) three different phases can be distinguished:

1. Failures right after construction
2. Failures within the normal use period
3. End of life failures

Failures right after construction are mainly due to construction mistakes. These mistakes are out of scope for this research. The failures within the normal use period are interesting, because condition assessments in this stage can be used as life-time prediction. It is a good practice to avoid sewer failure (e.g. collapsed sewer in figure 3.2) as significant associated effects can occur like: delays to traffic due to diversions, flooding of properties, public health consequences and environmental consequences (Davies et al., 2001).

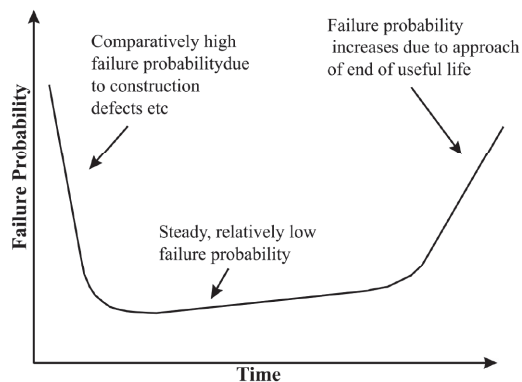


Figure 3.1: Bath tub failure curve of sewer pipes (Davies et al., 2001)

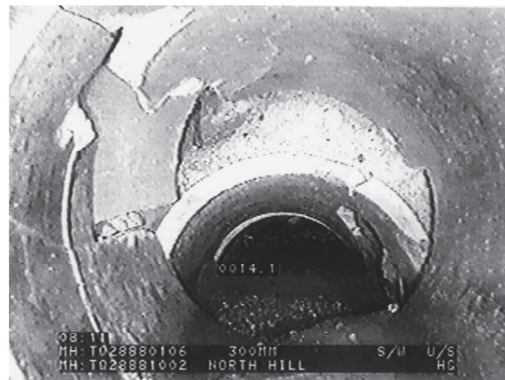


Figure 3.2: Camera image of a collapsed sewer pipe (Davies et al., 2001)

3.1.2 Failure process

The complete failure process of concrete pipes is always comparable independent of the cause. See figure 3.3: First the structural integrity is affected due to small crack. These cracks can be hard to visually observe due to dirt, some are even invisible because the pieces still align perfect. Under pressure, the cracks can split open and cause the pipe to slowly collapse. Even before collapsing, the sewer is not functioning optimally anymore. The sewer is not watertight anymore. To determine the condition of sewer pipes, it is important to be able to detect the start and progression of the failure process.

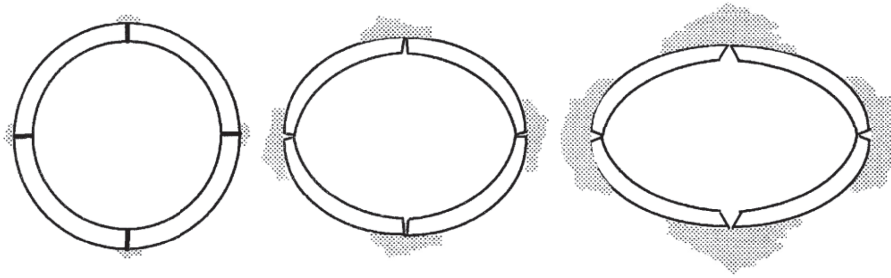


Figure 3.3: The failure process of a sewer pipe (Davies et al., 2001)

3.1.3 Condition aspects

By reasoning several important condition aspects are selected influencing the sewer failure. The quality and thus the strength of the concrete influences the condition too, this is however left out of scope.

- Concrete thickness (see experiment section 5.2)
Erosion occurs due to flow of water and dirt in the pipes. The sewer pipe wall thickness reduces, which influences the load bearing capacity of the pipe. Knowledge about the extent of pipe erosion will help determine the lifespan of the sewer pipe.
- Support material (see experiment section 5.3)
Cracks can cause sewer pipes to leak. The leaking fluids will flush away structures supporting these pipes. Air will replace the supporting soil. In combination with pressure from above, this increases the risk of the sewer collapsing.
- Flaw in concrete (see experiment section 5.4)
Loss of concrete can occur in sewer pipes due to cracks splitting open. This lack of concrete can occur at the outside of the pipe which is invisible from the inside. The structural integrity is affected and the pipe has an increased change of collapsing.

It should be kept in mind that condition assessment can only be performed relatively. The 'bad' spots in a sewer pipe can only be detected by comparing them to the 'good' spots. This is due to the non-destructive nature of the impact echo analysis. For absolute condition assessments only destructive measurements are applicable (Bungey et al., 2006).

3.1.4 Conclusion

Based on the analysis above the following condition determining aspects are selected to investigate further: Wall thickness, support material of the sewer pipe and missing concrete pieces of the pipe. With the assessment of these three aspects the condition can be determined. The concrete strength is left out of scope on purpose.

3.2 Condition influences on vibrations resulting from impact

This section discusses the influences of sewer pipe condition on surface vibrations after impact. It is strongly recommended to read section 2.1 first when unfamiliar with impact echo technology.

3.2.1 Concrete thickness

Concrete thickness is the first important factor to determine. The original thickness of the sewer pipe is approximately known and can therefore be used to verify if the measurements are performed correctly. Thickness (T) can be calculated when the P-wave speed (C_P) is known. As shown in figure 3.4, the frequency of the P-wave corresponds to the thickness. A frequency

peak at $1/\Delta t$ is expected in the frequency plot of the signal. The relation between T and Δt is shown in equation 3.1. β is a correction factor explained in section 2.1.2.

$$T = \frac{1}{2} \Delta t \beta C_P \quad (3.1)$$

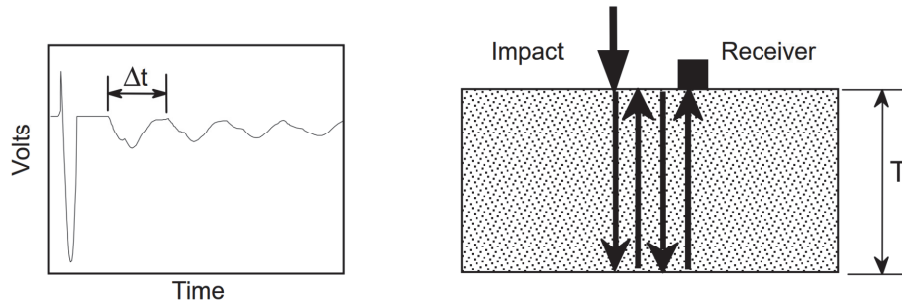


Figure 3.4: Thickness measurement of concrete after impact (Carino, 2001)

3.2.2 Support material

As explained in section 3.2.3 the support of the sewer pipe is important. To reduce the options, it is assumed that either sand or air support the pipe. Sand indicates a good condition of the support, air indicates a lack of support.

Air and sand have different reflection values (R). Air has an R -value of -1 and sand between -0.3 and -0.9 . This influences the amplitude of the reflection measured on the surface. Air causes the whole wave to reflect, whereas in sand the reflection is partly 'lost'. Although the difference might be small depending on the kind of sand, a slight decrease of amplitude of the thickness frequency is expected when sand is supporting the sample instead of air.

Detection of cavities around concrete sewer pipes with a surface mounted transducer is researched by Kang et al. (2017). They conclude air cavities are hard to detect using the Fourier spectrum especially for dry soils. Spectrogram analysis (short time Fourier spectrum) helps finding cavities and relative measurements are recommended.

3.2.3 Flaw in concrete

Delamination can cause flaws to arise in the concrete. A flaw indicates that the concrete is not a solid coherent substance anymore. There are two criteria used to detect flaws (Carino, 2015): The size (d) of the flaw (lateral dimensions of the reflecting interface) and the depth (T). Several scenarios are possible, these are shown in figure 3.5:

- (a) Solid concrete or $\frac{d}{T} < \frac{1}{4}$: There is no flaw or the size of the flaw is smaller than $\frac{1}{4}$ of the depth. There will be one peak for the thickness.
- (b) $\frac{1}{4} < \frac{d}{T} < \frac{1}{3}$: The size of the flaw is between $\frac{1}{4}$ and $\frac{1}{3}$ of the depth. The flaw can be detected, but the depth remains unknown.
- (c) $\frac{d}{T} > \frac{1}{3}$: The size of the flaw is larger than $\frac{1}{3}$ of the depth. The flaw and its depth can be detected
- (d) $\frac{d}{T} > 1.5$: The size of the flaw is larger than 1.5 times the depth. The response will be similar to a plate of the same thickness as the depth of the flaw.

For scenario (a) to (d) the frequency responses are shown in figure 3.5. (a) is the same as situation as discussed in section 3.2.1, the frequency peak is used as reference for the other scenarios. Flaws far underneath the surface or small flaws do not reflect enough to be detected, so

the response does not change. In situation (b) the flaw influences the thickness frequency, due to the longer distance that the diffracted waves travel. The waves reflected by the flaw do not contain enough energy to create their own frequency peak. The shift of the frequency peak indicates that there is a flaw, but the depth remains unknown. In situation (c) the received waves contain both frequency peak of the flaw and of the total depth of the sample. The thickness peak still shifts a little due to the diffracted waves. When the flaw is large or close to the surface (d), the frequency response is equal to a sample of the same thickness as the depth of the flaw. The low frequency peak f_{flex} corresponds to flexural vibration of the plate above the flaw. This so called "drum effect" is out of scope of this research.

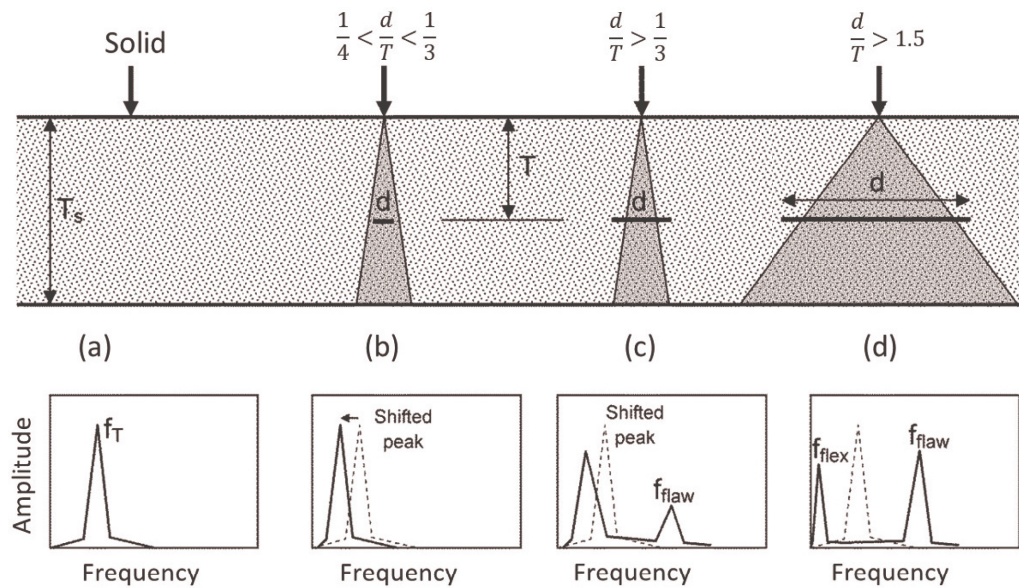


Figure 3.5: Scenarios for the depth and size of flaw in concrete (Carino, 2015). The cone in (b) and (c) represents $d/T = 1/3$ and the cone by (d) $d/T = 1.5$

3.2.4 Conclusion

As discussed in the above analysis, various conditions can be assessed using the frequency content of the reflected vibrations. The concrete thickness influences the vibrations in a clear way. The lack of support is harder to detect, because the difference in reflection ratio between sand and air is not large. Internal flaws are detectable depending on their depth and size.

3.3 Vibrations in concrete induced by impactor

3.3.1 Frequency content

'Impactor' refers to the object hitting the surface. In general metal balls are used as impactors to generate waves in concrete. A ball is symmetric in all directions and therefore creates a uniform wave in all directions. The size of the ball influences the impact time. The larger the diameter of the ball (D), the longer the impact time (t_c). The impact time for a steel ball dropping on a concrete surface is approximated by $t_c = 0.0043 \cdot D$ and the maximum frequency (f_{max}) transferred to the concrete by $f_{max} = \frac{1.25}{t_c}$ (Colla and Lausch, 2003).

The shorter the impact duration, the larger the frequency range of waves generated in the object (Colla and Lausch (2003)). This is clearly illustrated by figure 3.6. If the impact time (t_c) is shorter, the signal contains higher frequencies. This is important, because the frequencies of the waves generated in the concrete influence the depth which can be measured.

The frequencies excited in the concrete should be higher than the frequencies that you want to use in the analysis of the concrete. In this case, the thickness frequency as discussed in

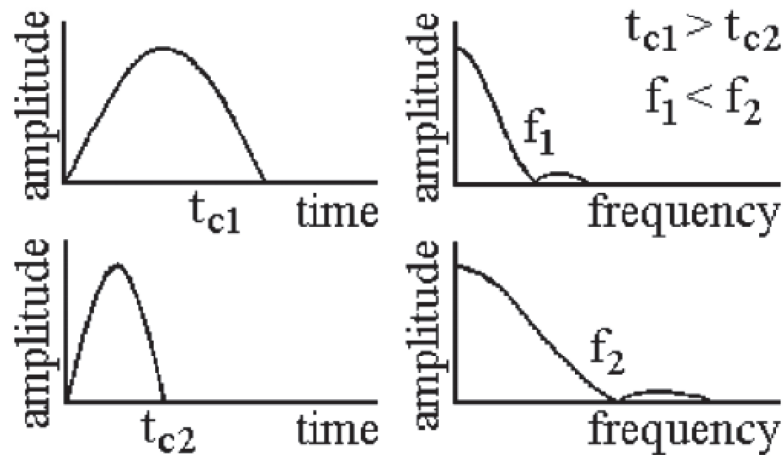


Figure 3.6: Relation between impact contact time t_c (left) and frequency range f of the wave (right) for the case of longer (above) and shorter t_c (below). Colla and Lausch (2003)

section 2.1.2 is decisive. When the frequency is too low, the relevant frequency peaks cannot be detected. When the sample thickness is known, the appropriate impactor diameter can be selected. A smaller impactor always works, however it becomes harder to generate waves with an adequate amplitude which is discussed in the next section.

3.3.2 Amplitude influence

The impact force determines the amplitude of generated waves. Noise will dominate the measured signal if the force is too low. On the other hand, the test will become destructive for the material when the used force is too high. Exact impact force values are unavailable from literature because, in current practices, the impact is mostly generated by an operator using a steel bell on a rod. The measured amplitude of the surface vibrations is therefore used to determine the required force. When the amplitude of the reflections is too low, the impact force should be increased.

The sound source area (explained in section 2.2) is influenced by the amplitude of the generated waves. The vibrating area of the surface will increase if the force that is transferred in the impact increases.

It is harder to generate vibrations with a high enough amplitude without damaging the surface for small impactor sizes. If the contact area is too small, the local stress might exceed the elastic deformation boundary.

3.3.3 Conclusion

Based on the above analysis, we conclude that the minimum expected thickness (or depth of an internal flaw) determines the required maximum contact time and therefore the size of the impactor. The impactor ball can always be made smaller, but it becomes harder to generate vibrations with a large enough amplitude without damaging the material.

3.4 Measuring vibrations contactless with particle velocity sensor

3.4.1 Particle velocity sensor

A particle velocity sensor of Microflown is used. The Microflown is invented in 1994 at the University of Twente (the Netherlands). It is composed of two heated extremely thin wires. Particles passing the wires change their temperature and therefore the resistance. A particle velocity signal passing cools the upstream wire more than the downstream wire. The resistance

difference provides a broadband (approximately 0 Hz to 10 kHz) linear signal with a figure of eight directivity (Raangs, 2005). A disadvantage of this measuring method is the sensitivity to other particle flows than sound, such as wind. However, since sewer inspection are done in sealed pipes, this should not be a problem.

The response of the sensor can be linearized up to 20 kHz when the provided correction filter is used, gain and phase for higher frequencies are not specified. To determine if the particle velocity sensor can measure higher frequencies at all, a simple experiment is executed (see figure 3.7a): The particle velocity sensor is placed in front of a speaker which is connected to a waveform generator (Agilent 33220A). Various frequencies of sine waves are tested and the measured results are shown in figure 3.7b. Even at 20 MHz the signal is still received - although at a low amplitude - in good quality. The signal of 20 kHz is very distorted. This causes no problem since we will be using the signal for frequency analysis and the main present frequency is still 20 kHz when looking at the frequency content. There are several causes possible for, but those are out of scope of this research. The 50 kHz response looks angular at some points, this is not due to aliasing, but the reason remains unknown. The conclusion from this small check is: The used particle velocity sensor is able to measure signals with higher frequencies than 20 kHz, however the exact gain and phase remain unknown.

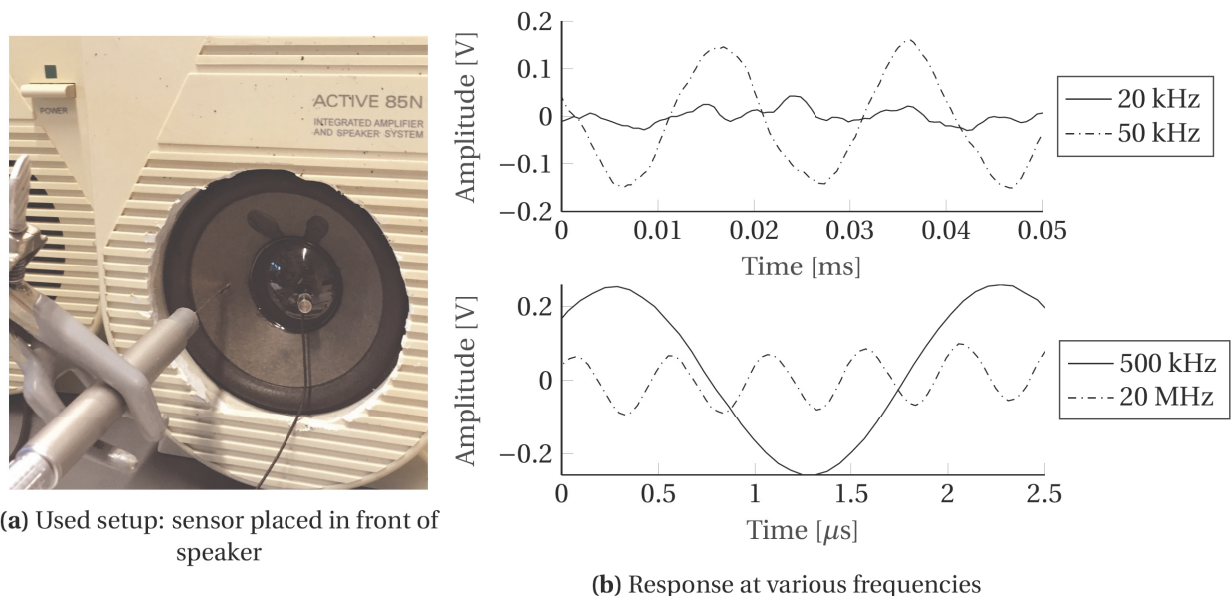


Figure 3.7: Frequency response test of Microflown U Regular

3.4.2 Sensor placement

It is strongly recommended to read section 2.2 first when unfamiliar with the very near field effect. The vibration of the concrete is transmitted to the surrounding air particles. These vibrations are measured with a particle velocity sensor. When measuring in the very near field this sensor should be able to measure the surface vibrations with less influence of background noise compared to a pressure microphone, which is an advantage.

The height above the vibrating surface is determined by the very near field. In order to measure in the very near field the sensor should be placed in the very near field. The very near field is influenced by the size of the vibrating surface, the sensor should be closer than the size of the vibrating object divided by 2π . The size of the vibrating surface also determines which frequencies are in the very near field: the wavelength of the wave should be larger than the vibrating surface. The size of the vibrating surface is effected by the impact force, the larger the force, the larger the vibrating surface.

The placement of the particle velocity sensor compared to the impact point is determined by guidelines. The vibration receiver should be placed between 20 % and 50 % of the distance to the closest reflection point in the material (Carino et al., 1986). In this way both unwanted influences of the large R-wave amplitude and S-wave reflections are minimised.

3.4.3 Conclusion

From the discussion above we conclude that the following aspects need to be considered when measuring the vibrations contactless using a particle velocity sensor. The sensor should be placed close to the surface in order to be in the very near field and reduce the background noise influence. The frequencies that benefit from this background noise reduction are limited by the sound source size. In order to measure the correct reflected waves from the impact, the sensor should be placed between 20 % to 50 % of the distance of the closest expected reflection point in the material under inspection.

4 Experimental setup

In chapter 3 information about interesting condition aspects and how to assess them is discussed. In this chapter the experimental setup made with the knowledge of the analysis is presented. In figure 4.1 a schematic overview is shown of the experimental setup. All parts are discussed in this chapter and at last the total experimental setup is displayed.

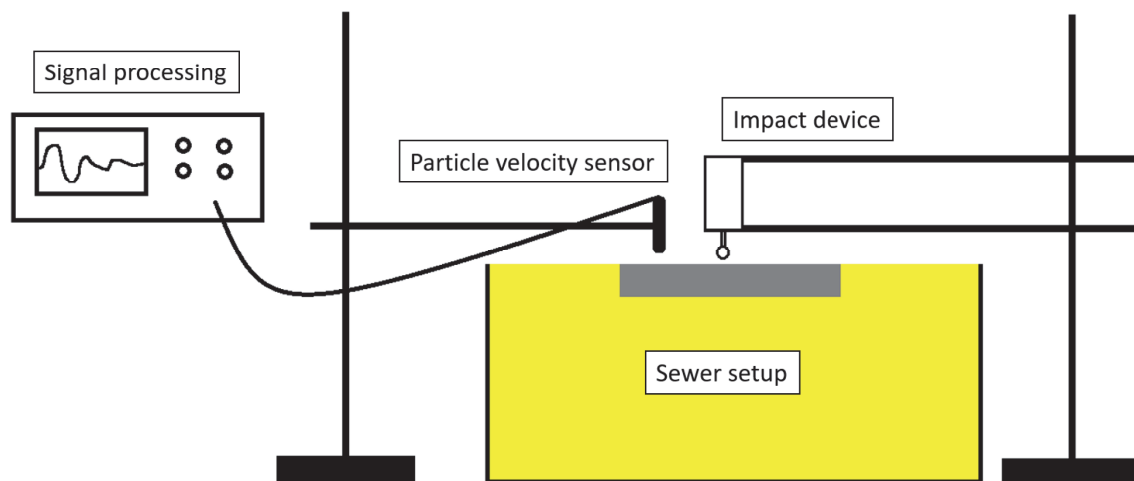


Figure 4.1: Schematic overview of experimental setup

4.1 Sewer setup

In order to mimic the sewer environment in a lab setup, it is chosen to use concrete tiles supported by sand. This is a simplified setup compared to a real sewer pipe, however more manageable than curved structures supported with varying compositions of soil.

The tiles are available in various thicknesses and are all made of solid concrete. A tile is like a rolled-out sewer pipe. Samples required for examining all described condition determining aspects of section 3.1 can be created using tiles.

The floor tiles are displayed in figure 4.2. All tiles have an identical top area and are available in four different thicknesses. See table 4.1 for more details about the dimensions.

Sample name	Actual thickness [mm]	Top surface LxW [cm]	Weight [kg]
4 cm	41	30 × 30	8.8
4.5 cm	46	30 × 30	9.4
6 cm	59	30 × 30	12.4
8 cm	83	30 × 30	17.1

Table 4.1: Sample dimensions

The producer does not provide all specifications of the concrete, therefore some properties are assumed. In table 4.2 the assumed material properties are shown. The correction factor β is based on Gibson and Popovics (2005). With these assumed properties the P-wave speed can be calculated using equation 2.1, which is $2.8 \times 10^3 \text{ ms}^{-1}$. This is an assumed value, in reality the P-wave speed can deviate quite a bit, influencing all calculations. During the analysis of the experiment results, the real P-wave speed can be determined using the real sample thickness.

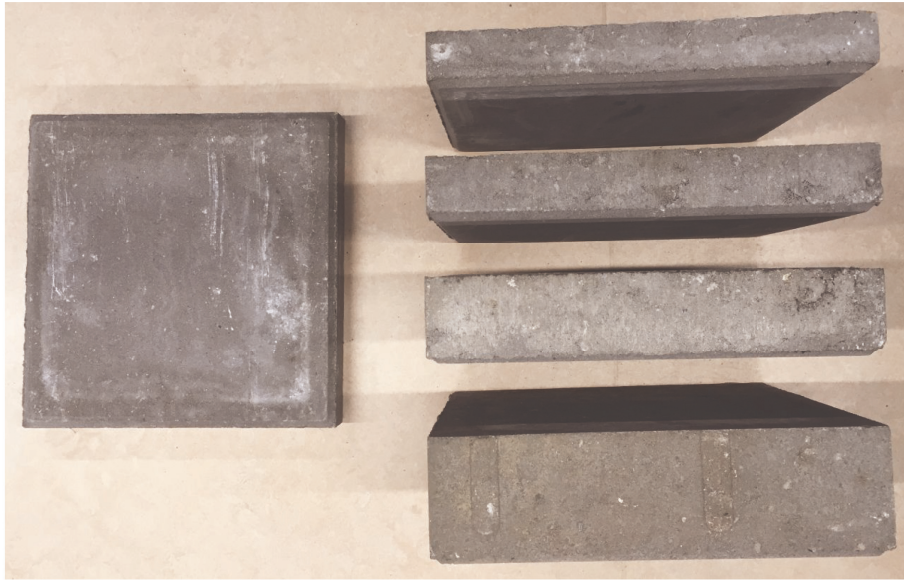
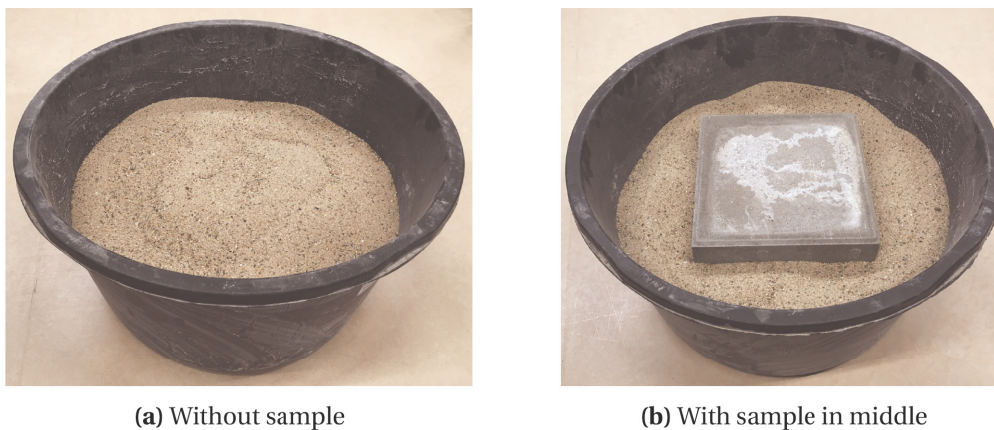


Figure 4.2: Identical top of all samples (left). All available thicknesses (right).

Young's modulus	E	17 GPa
Density	ρ	2400 kgm ⁻³
Poisson's ratio	ν	0.18
Correction factor	β	0.955

Table 4.2: Assumed material properties of concrete tiles

A 90 L mortar tub is filled for two-thirds with sand (see figure 4.3a). This setup is chosen to mimic the support of a concrete sewer pipe. In real life the sand can be wet. However, when using wet sand it is hard to keep the moisture level constant throughout all the experiments. Keeping the support constant during all experiments is important, because the humidity influences the reflection ratio of the sand.



(a) Without sample

(b) With sample in middle

Figure 4.3: Tub for sample support

The tub has a diameter of 61 cm and is 35 cm high. The sand composition is measured using a sieve analysis. The sand composition is summarised by the D-values: D10 = 0.25 mm, D50 = 0.52 mm and D90 = 1.4 mm. The D10 = 0.25 mm means: 10 % of the total mass of the sand passes through a sieve with holes of 0.25 mm diameter. The exact contents and derivation of the D-values can be found in appendix A.

The samples will be placed in the middle of the tub on top of the sand (as in figure 4.3b). It is important that the tile is in full contact with the sand, so no air cavities exist. Air cavities will influence the measurements, so they should only exist when intended.

4.2 Impact device

To be able to deliver an identical impact for all experiments, an impact device is designed. By combining a solenoid, micro controller and several sensors, a device that can also be used for further research is created.

4.2.1 Force generation

The impact force is generated by a solenoid. Because the solenoid itself will also endure impacts, a non-magnetic core model is chosen (ITS-LS 5852 of Red Magnetics). A magnetic core would lose its magnetic properties over time due to the impacts. The non-magnetic core solenoid can only exert force in one direction. Retraction is done by a spring. The solenoid can deliver an average of 59 N over a stroke of 30 mm, with results in $E_{kin} = F \cdot s = 59 \cdot 0.030 = 1.77 J$. This is a large impact, since there are destructive rotary hammers for sale with less impact energy. Because the tests should remain non-destructive, probably not all force off the solenoid is needed. The solenoid weighs about 1 kg.

4.2.2 Impactor

As impactor a steel sphere is used. The maximum diameter of the sphere (D) is determined by the frequency required for the thinnest sample (see the equations in section 3.3). The thinnest sample is 41 mm (T). The assumed P-wave speed (C_p) is $2.8 \times 10^3 \text{ ms}^{-1}$, but to ensure the frequency content is sufficient, it is taken to be the maximum expected value of 4000 m s^{-1} .

$$D = \frac{2T}{C_p \cdot 0.0043} = \frac{2 \cdot 0.041}{4000 \cdot 0.0043} = 4.8 \text{ mm} \quad (4.1)$$

A diameter of 4.5 mm is chosen during the production as this is commercially available. The impact time should be $t_c = 0.0043 \cdot D = 0.0043 \cdot 0.0045 \approx 20 \mu\text{s}$.

4.2.3 Actuation control

Control hardware

The solenoid is powered with 70 V switched by a high voltage transistor. The back electromotive force generated by the solenoid after powering it is handled using a Transient-Voltage-Suppression (TVS) diode as flyback diode. To adjust the solenoid force, the transistor is controlled by a PWM (Pulse-Width Modulation) signal. An Arduino Micro (16 MHz clock speed) is used to generate the PWM signal and handles all other inputs and outputs. For user input five buttons are mounted and a display is installed to give feedback. The circuit connecting all parts is found in appendix B.

The Arduino program lets the user select the PWM duty cycle (0 – 255) and set the time the solenoid is powered in milliseconds. The settings are displayed on the display. When the impact button is pressed, the impact is generated with the defined settings. The code is found in appendix C.

Actuation settings

The settings for the impact generation are set by trial-and-error. The impact should be firm and only hit the surface once. The distance between the impactor and concrete is set to 14 mm (see figure 4.4) and PWM to maximum power (255). Now the powering time of the solenoid is increased until the surface is hit firmly. With a high-speed camera it is verified the surface is only hit once. This resulted in a power time of 21 ms.



Figure 4.4: Distance between impactor and surface

4.2.4 Sensors

Force sensor

The impactor is equipped with a force sensor for several reasons: To get an idea of the impact energy, to verify the contact time and to locate the interesting data in the surface vibration data set.

A FlexiForce Sensor (type A201) is chosen, which is a force depending resistance. It is mounted in line with the impact (see figure 4.5) such that only the force exerted on the surface is measured. Forces up to 4000 N can be measured (Tekscan, 2018).

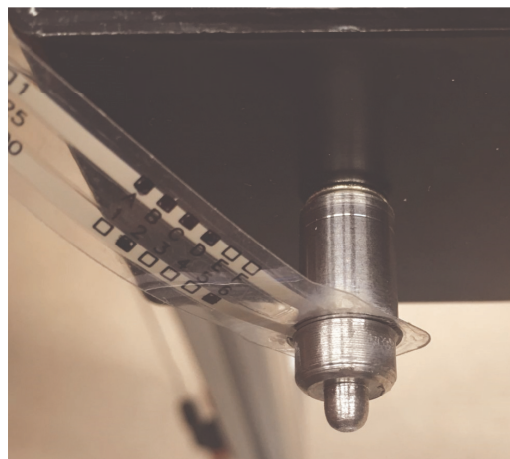


Figure 4.5: Force sensor for impactor

The relation between resistance and force is determined through calibration. The force sensor is calibrated using a scale, see figure 4.6. The weight can be translated to a force. This way the output signal of the sensor (0 V to 5 V) can be linked to an actual force. The sensor output is measured using an oscilloscope.

The calibration measurements and linear curve fit are shown in figure 4.7. During calibration a maximum force of approximately 500 N was applied. Higher static forces were inconvenient to place on top of the solenoid core. With the formula of the fitted curve, the impact voltage measurements can be translated to forces.



Figure 4.6: Force sensor calibration setup using scale

Additional sensors for future purposes

For further research purposes various sensors have already been included in the design. During actual sewer inspection, measurements should be carried out all around the sewer. To determine the orientation of the impactor a nine degree of freedom IMU (3-axis accelerometer, 3-axis gyroscope, and 3-axis magnetometer) is included. In order to position the impactor at the correct distance to the concrete a distance sensor (time of flight) is added as well. These sensors are present, but not used during this research.

4.2.5 Total impact device

The total overview of the device is shown in figure 4.8. It will be fixed to a frame above the samples. The Arduino power connection requires 9 V DC (250 mA or more). It is not advised to supply the solenoid power connection (XT60) with more than 100 V.

The impactor is placed such that it impacts the samples in the middle. This way the distance to the edges of the tile is the longest for all directions, so that the influences of these reflections is minimised.

4.3 Particle velocity sensor

A particle velocity sensor of Microflown (type U Regular) is used to measure the surface vibration in combination with the corresponding signal conditioner of Microflown (type E0906-52). The particle velocity sensor is placed 20 mm from the impact point. For the thinnest sample (41 mm thick) this is $\frac{20\text{mm}}{41\text{mm}} = 49\%$ of the distance to the closest reflection. For the thickest sample (83 mm thick) this is $\frac{20\text{mm}}{83\text{mm}} = 24\%$. This is according to the guideline (see section 3.4.2) of placing the sensor between 20 % to 50 % of the distance to the closest reflection.

The distance between the concrete and particle velocity sensor is determined by the very near field effect (see section 2.2). If it is assumed that the whole tile surface vibrates, the source size L is 30 cm. The sensor should be positioned closer than $\frac{30\text{cm}}{2\pi} = 4.77\text{ cm}$. It is however unsure if the whole sample surface will vibrate. To ensure we are measuring in the very near field, the sensor distance is lowered to approximately 1 cm. To avoid accidental collisions with the surface the distance is not lowered further.

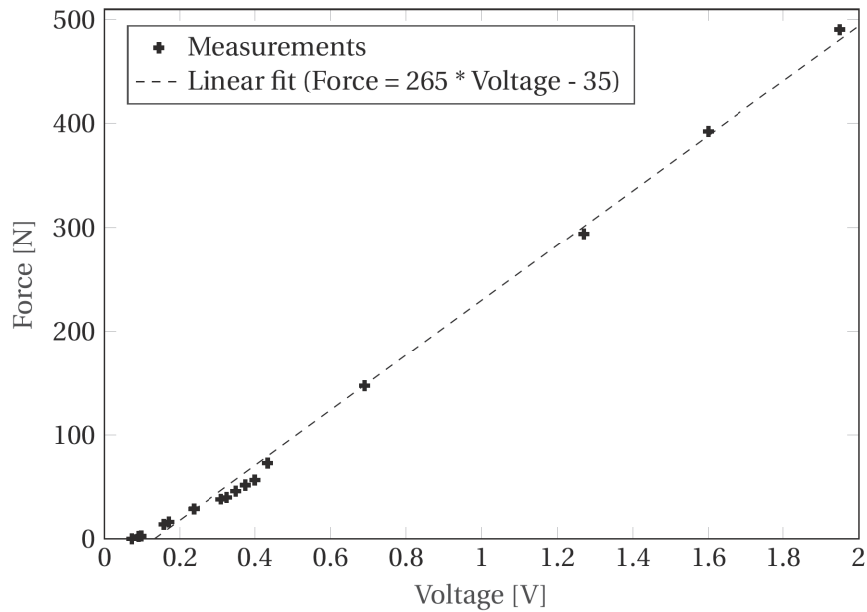


Figure 4.7: Calibration of force sensor: measurements and linear curve fit

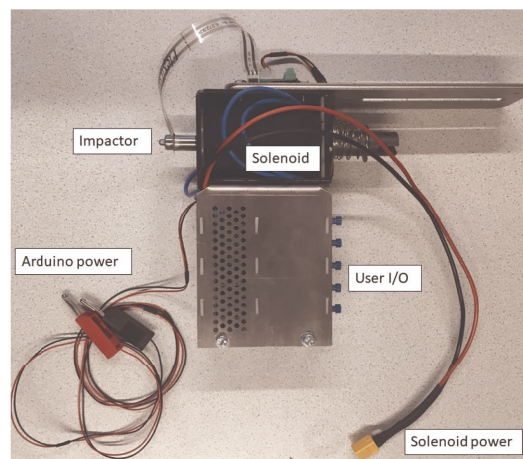


Figure 4.8: Overview of total impact device

The higher frequencies are not in the very near field due to the wavelength compared to the vibrating surface. The higher the frequency, the smaller the wave length. The wave length should be larger than the vibrating object size. When the same assumption about the source size is made, frequencies higher than approximately $\frac{C_{air}}{\lambda} = \frac{343}{0.30} \approx 1150 \text{ Hz}$ are not measured in the very near field. C_{air} is the wave speed of air in ms^{-1} . Frequencies higher than 1150 Hz are more influenced by background noise.

4.4 Signal processing

All data is logged using an oscilloscope (Rhode&Schwarz RTB2004) which has a bandwidth of 300 MHz. The data is further analysed using MATLAB, resulting in figures suitable for frequency analysis. The data processing algorithm is built up as follows:

1. Load the comma-separated values from the oscilloscope. These contain the voltage of the particle velocity sensor, force sensor and eventual microphone for all time instances.
2. Search the impact using the force-data. The data contains more than pure the impact vibrations. Ignore voltage peaks due to solenoid powering and back electromotive force.

3. Split data in:
 - (a) Vibrations of 2 ms after impact without the R-wave.
 - (b) Background noise for reference. A sample with the same length is taken of the data before the impact. This way the impact vibrations can be compared with the background noise.
4. Execute FFT (Fast Fourier Transform) on both the 'vibrations after impact' and the 'background noise'. The frequency content of each sample is determined.
5. Each test is conducted several times, the average in the frequency domain is calculated.
6. Calculate the minimum and maximum amplitude of each frequency for each set of tests. This gives an idea of the variance between test of the same situation.
7. Plot the results, see figure 4.9 as example:
 - (a) Average of frequencies after impact
 - (b) Minimum - maximum area of the frequencies after impact
 - (c) Average background noise level
 - (d) Expected frequency peak for comparison

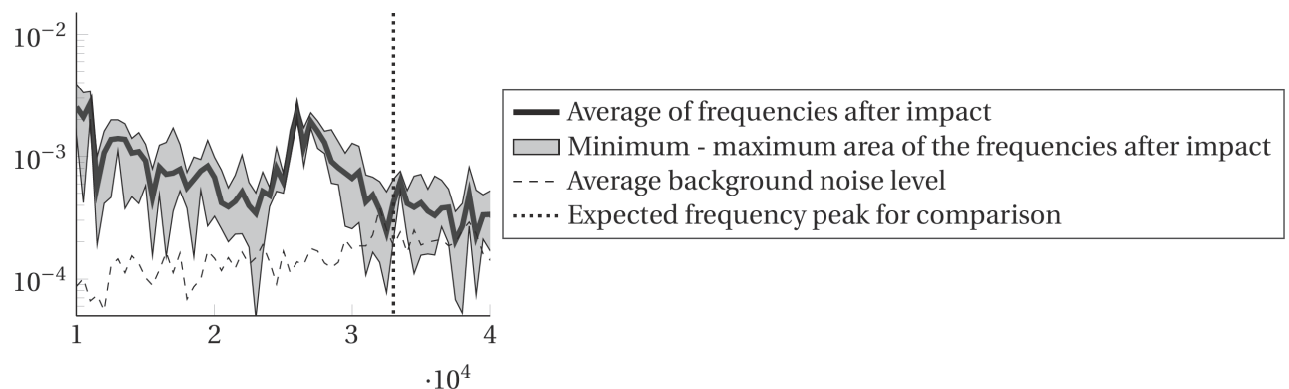


Figure 4.9: An example of the plotted data

Only the frequency content between 10 kHz to 40 kHz is considered. This range is chosen because the expected peaks (explained later for each experiment) are within this range. Lower frequencies are a combination of reflection as well as the sound induced by the impactor itself. Higher frequencies cannot be given a physical meaning without thorough finite element simulation.

4.5 Total setup

In figure 4.10 the total setup is displayed: The sample is in the tub with sand. The particle velocity sensor is fixed by a tripod. The impactor device is suspended by a frame. Both are consciously not mounted on the same frame in order to avoid unintended vibrations measured by the particle velocity sensor.

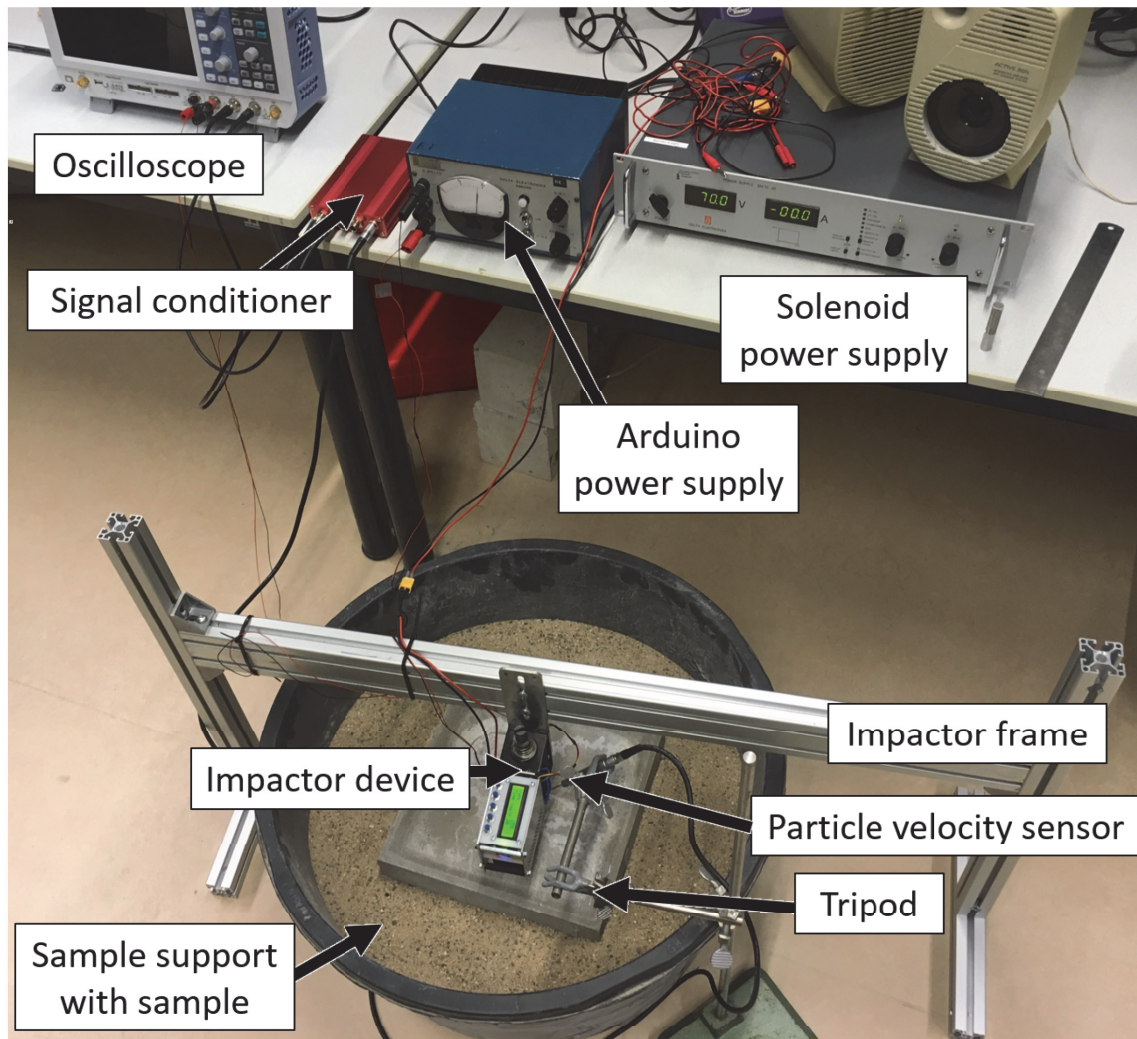

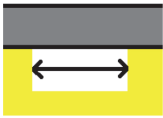


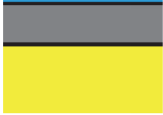


Figure 4.10: Overview of the total experimental setup

5 Experiments

In this section, experiments to evaluate if the desired setup can be used to distinguish between good sewer pipes and pipes in poor condition are conducted. An overview of all different experiments is shown in table 5.1. Each experiment is discussed in a separate section. All different tests in this chapter are executed five times.

Table 5.1: Overview of the experiments

Section	Experiment	Description
5.1	Validation of setup	In order to verify the created impact device some tests are performed. The impact time and force are important, see section 3.3.
5.2		In order to determine the amount of erosion and to verify if the measurements are conducted correctly, samples with various thicknesses are tested. The thickness frequency should change with the thickness as discussed in section 3.2.1.
5.3		Lacking support of the sewer increases the change of collapsing. To check if a cavity in the support can be detected various sizes of cavities in the support are tested. This a challenging according to section 3.2.2.
5.4		A flaw in the concrete is mimicked with a cavity in the concrete. Various sizes of cavities are tested. The size-depth ratio determines if the flaw is detectable, see section 3.2.3.
5.5		To verify if and to what extent the background noise cancellation property of a particle velocity sensor (see section 3.4) works, various levels of background noise are generated. The particle velocity sensor is compared with a normal pressure microphone. It is expected that the particle velocity sensor can still measure the surface vibrations in the presence of loud background noise.
5.6		Because a sewer is a wet environment, it is tested if the condition assessment is also possible when there is water on the surface or if the concrete is saturated with water.

All experiment are discussed in the same way:

1. Motivation: The reason for conducting the experiment is discussed. This is closely linked to the sewer condition determining aspects (see section 3.1).
2. Experiment design: The exact experiment setup - with all tested situations - is explained.
3. Hypothesis and calculations: With the analysis chapter in mind, a hypothesis is formulated. When possible, the expected outcomes are calculated.
4. Results: The results are shown and discussed.
5. Discussion: The results are compared with the hypothesis and calculated expectations
6. Conclusion: The conclusions drawn from the experiment are summarised.

5.1 Validation of setup

1. Motivation

In order to conduct impact echoes in the correct way, the contact time is important. When the contact time is too long, results of all experiments will be influenced negatively.

Although not used in this research, the impact energy is calculated because this might be interesting for further research.

2. Experiment design

The 8 cm thick tile is impacted with the settings mentioned in section 4.2.3.

3. Hypothesis and calculations

The impact time should be $t_c = 0.0043 \cdot D = 0.0043 \cdot 0.0045 \approx 20 \mu\text{s}$ (see section 3.3). The real impact time can be derived from the force sensor (see section 4.2.4).

The solenoid is only powered for a short time, so a low impact energy is expected. The impact energy can be calculated using the force-time data of the impact. It is assumed that the impact energy is equal to the kinetic energy of the impactor. The mass m of the impactor is known (142 g). The velocity needs to be extracted from the force-time data in order to calculate the kinetic energy $E_{kin} = \frac{1}{2}mv^2$.

$$\text{Impulse} = \int F dt = m \cdot \Delta v \quad (5.1)$$

This can be rewritten to:

$$\Delta v = \frac{m}{\int F dt} \quad (5.2)$$

$\int F dt$ is equal to the area under a force-time diagram. Δv is the difference in speed between the concrete surface and the impactor. Since the concrete does not move, Δv is equal to the speed of the impactor v only. The impact energy can now be calculated using:

$$E_{kin} = \frac{(\int F dt)^2}{2m} \quad (5.3)$$

4. Results

In figure 5.1 the force during an impact is displayed.

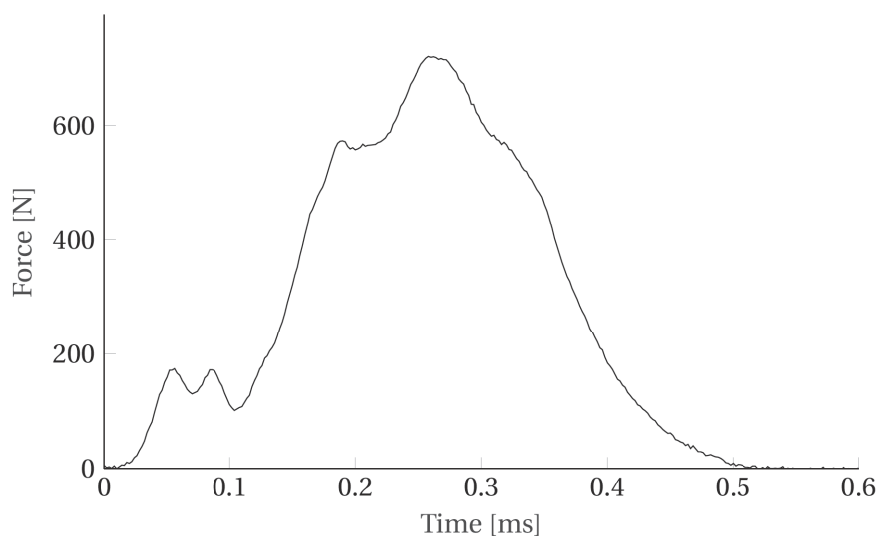


Figure 5.1: Force during impact

The force increases with some small bumps up to 720 N and decreases back to zero after reaching the maximum. The total time force is exerted is approximately 500 μs .

5. Discussion

The contact time is 25 times too long. The higher frequencies - which are interesting - are damped in the concrete. To verify if this was due to the low retraction force of the spring, the impact is also checked when the impact device is upside down. This way the gravity pulls the impactor down. The impact time was even longer, so the retraction force is not the issue.

The assumption about the contact time is wrong. The formula used was for dropping a steel ball with a certain diameter. The designed impactor has an increased inertia compared to a steel ball, therefore the contact time is longer.

In order to calculate the impact energy $\int Fdt$ needs to be defined. In figure 5.2 the impact impulse area is shaded. The force-time plot consists of two parts: an impulse and rebound. The concrete can be seen as spring; the force increases when the displacement increases. At the maximum force the potential energy of the 'concrete spring' is the largest and the rebound begins. Because only the impact energy is of interest - and not the rebound energy - only the shaded area is used for the impact energy calculation

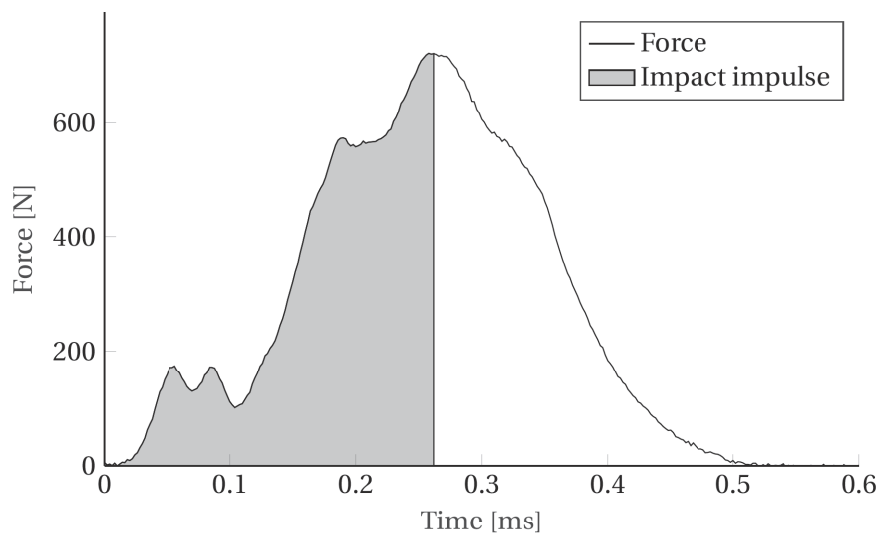


Figure 5.2: Impulse during impact

With equation 5.3 and the shaded area of figure 5.2, the impact energy is calculated and equals 0.024 J.

6. Conclusion

The contact time of the impactor is significantly too long, due to a wrong assumption. All expected frequency peaks will be damped and less visible in analysis. The impact energy of an impact is approximately 0.024 J.

5.2 Varying thickness

1. Motivation

The thickness of a sewer pipe is interesting to detect, see section 3.1. Testing the thickness gives an indication of its wear, but also verifies if the tests are conducted correctly.

2. Experiment design

Samples with varying thickness (other dimensions should be the same) are tested. Three are selected: 4 cm, 6 cm and 8 cm thickness. All samples are excited in the middle with the same impact. The samples are in full contact with the sand.

3. Hypothesis and calculations

The hypothesis in this experiment is a clear frequency peak for the thickness frequency. The peak of the thicker tiles should be lower in the frequency domain. It is expected that the thinnest sample has a thickness frequency out of the linear range of the sensor. Due to the too long contact time of the impactor, thickness frequency peaks might be damped.

The expected thickness frequencies are calculated using the formula from section 2.1.2. The P-wave speed C_P is estimated in section 4.1.

$$f_T = \frac{\beta C_P}{2h} = \frac{0.955 \cdot 2800}{2h} \quad (5.4)$$

- 4 cm sample: Actual thickness is 41 mm, so the peak is expected at 33 kHz.
- 6 cm sample: Actual thickness is 59 mm, so the peak is expected at 23 kHz.
- 8 cm sample: Actual thickness is 83 mm, so the peak is expected at 16 kHz.

Because the P-wave speed (C_P) and the correction factor β are assumed, the measured peaks might differ. The difference between varying thicknesses should still change in relation to the thickness.

4. Results

The results of this experiment are shown in figure 5.3. For the 8 cm thick tile a clear peak can be

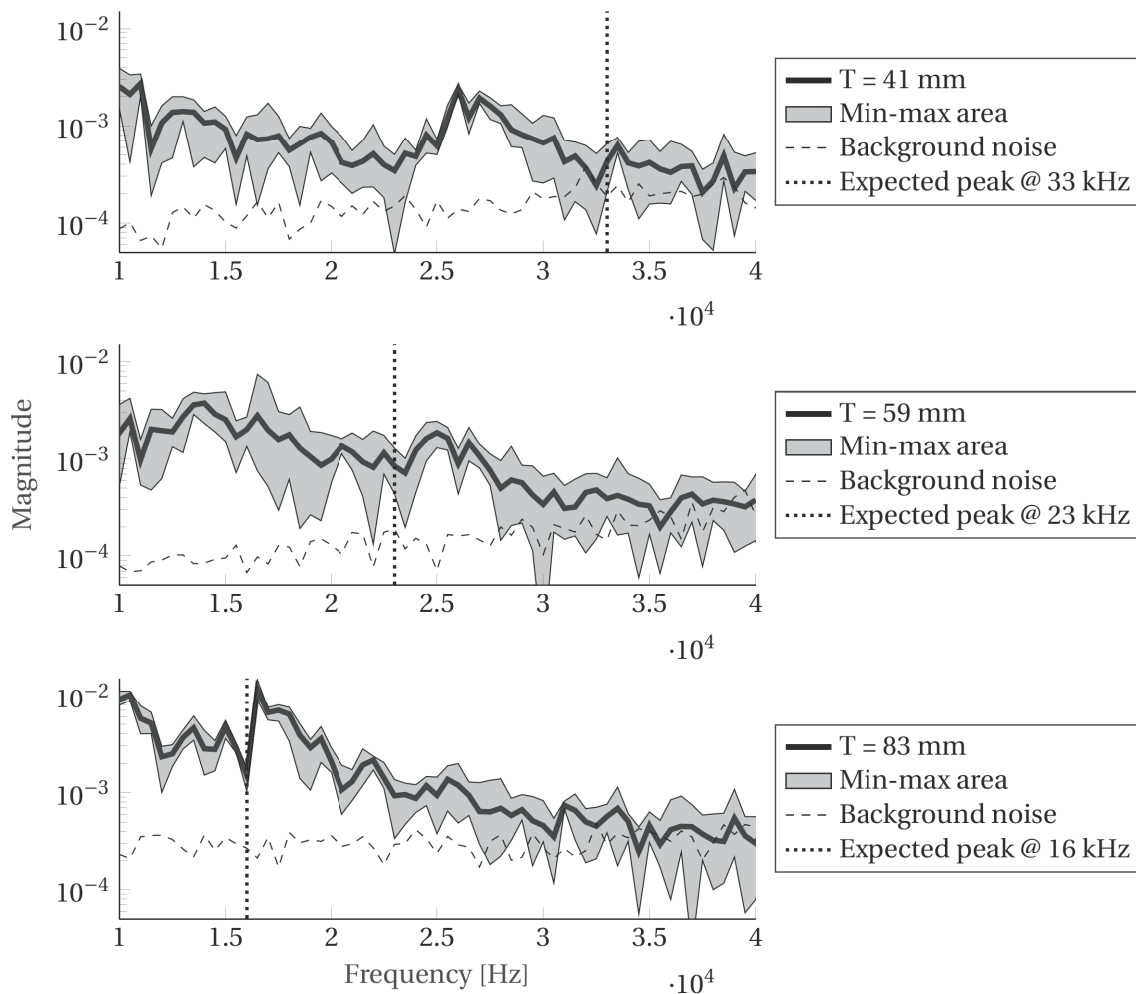


Figure 5.3: Frequency plots of impact echo on the 4 cm, 6 cm and 8 cm thick samples

seen at 16.5 kHz. The 6 cm thick tile results show plenty local peaks, but no global outstanding one. The 4 cm thick tile shows a peak at approximately 26 kHz.

The min-max areas are also plotted on logarithmic scale. This can be misleading in the variance judgement. In figure 5.3 it looks as if near the expected thickness frequency peaks the variance is very little, especially for the 4 cm and 8 cm thick tiles. In fact, there is no distinguishable lower variance at these points.

For frequencies higher than 30 kHz the background noise level is comparable to the impact signal level. For lower frequencies the difference between noise and impact vibrations is clear.

5. Discussion

The expected thickness frequencies are also plotted in figure 5.3. For all samples the expected peak frequency is compared with the real peak in table 5.2. The closest visible peak is assumed to be the real peak. The peak is global if it has the largest magnitude in the 10 kHz to 40 kHz range. With the help of equation 5.4, the P-wave speed is recalculated. It is assumed that the correction factor β remains the same.

Table 5.2: Thickness frequencies results

Sample name	Expected peak	Real peak	Global or local	P-wave speed
4 cm	33 kHz	33.5 kHz	Local	2880 ms ⁻¹
6 cm	23 kHz	25 kHz	Local	3090 ms ⁻¹
8 cm	16 kHz	16.5 kHz	Global	2870 ms ⁻¹

Only the 4 cm thick sample shows a global peak within the shown frequency range. This makes sense since the particle velocity sensor has a linear response up to 20 kHz in combination with the signal conditioner. Higher frequencies have a lower gain, but since the sensitivity for these frequencies is unknown they cannot be corrected. Despite the lack of global peaks close to the expected values, for both tiles a local peak close to the expected frequency was present. With local peaks it is impossible to reverse the analyses process, so the thickness of an unknown sample cannot be detected for thin samples.

A new P-wave speed can be calculated for further experiments. From the three P-wave speeds in table 5.2 one is odd: 3090 ms⁻¹ differs slightly from the others. The new assumed P-wave speed will be the average of the calculated speeds all samples: 2945 ms⁻¹.

It is unclear where the high peak at 26 kHz for the 4 cm thick sample originates from. It is not close to the expected value.

The small difference in magnitude between impact vibrations and noise for frequencies higher than 30 kHz makes well substantiated conclusions for peaks in that range hard. This is another reason to avoid assessment of thin structures.

6. Conclusion

For the 8 cm thick tile it was possible to detect its thickness due to the global peak. It is expected that samples with a thickness frequency up to 20 kHz can be measured. The frequency peak for the 8 cm thick tile has a large variance. For the thinner tiles no global peak was seen, probably due to the lower sensitivity for higher frequencies of the particle velocity sensor. For further experiments the P-wave speed for calculations will be assumed to be 2945 ms⁻¹. The 8 cm thick tile is used in further experiments to avoid linear sensitivity limits of the particle velocity sensor and have a clear difference between noise and reflected vibrations.

5.3 Varying cavity support

1. Motivation:

A cavity in the support of the sewer pipe suggests a poor condition of the pipe. Support cavities are hard to detect, but the vibration reflections are still interesting. It is assumed that these cavities are filled with air. The size of the cavity is varied to investigate its influence.

2. Experiment design

The 8 cm thick tile is used in this experiment due to the lowest thickness frequency. The frequency response of a fully supported tile is compared with several size of cavities in the support (see figure 5.4). The cavity is made by removing sand in the middle in a circular way using a mould of the correct diameter. To avoid influence of the mould it is ensured it does not touch the sample. The diameters of cavities tested are 5 cm, 10 cm and 15 cm.

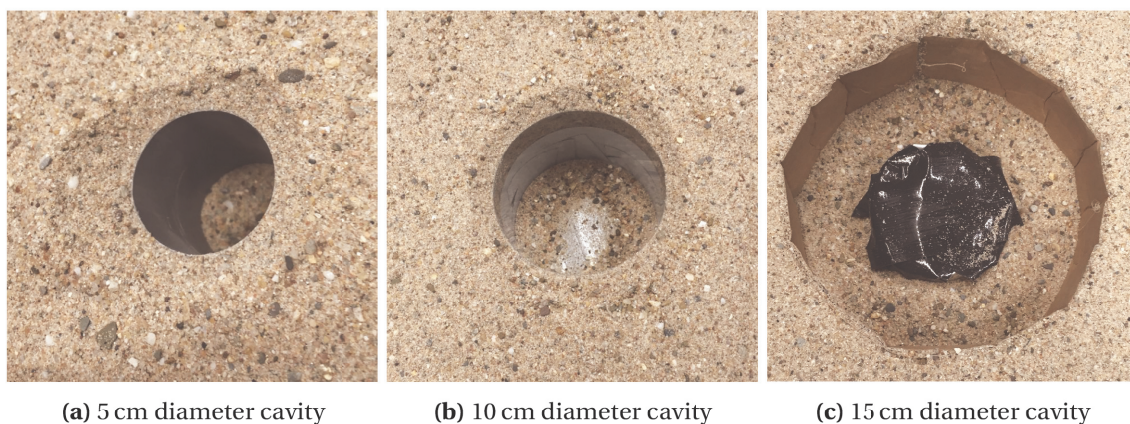


Figure 5.4: All artificial created cavities in the sample support

3. Hypothesis and calculations

Due to the difference in reflection ratio between sand and air, it is expected that the thickness frequency peak of the concrete increases slightly in amplitude (see section 3.2.2). If the cavity is bigger, the amplitude should increase even more. This is because air reflects 'perfect' and sand only reflects the P-wave partial. The frequency of the thickness frequency should not change significantly. It is however expected that the differences are hard to notice, because dry soil is used, which is challenging according to Kang et al. (2017).

Sand has a reflection coefficient between -0.3 and -0.9 with concrete and air reflects the P-wave fully (coefficient is -1). The reflection theory therefore suggests that the samples with air cavity show a 10% to 70% increased amplitude for the thickness frequency peak. These percentages are only if the whole P-wave reflects on the air cavity, otherwise the increase is less.

The expected thickness frequency using the new assumed P-wave speed of 2945 m s^{-1} (using equation 5.4) is 16.9 kHz.

4. Results

In figure 5.5 the results for various sizes of cavities are shown. The first plot of the 'No cavity' samples is copied from the previous experiment as reference. The results show a comparable response for all samples with support cavities. Around 16.9 kHz all situations show a small peak, but the amplitude does not stand out compared to the other peaks. The whole response is flat compared to the sample without support cavity.

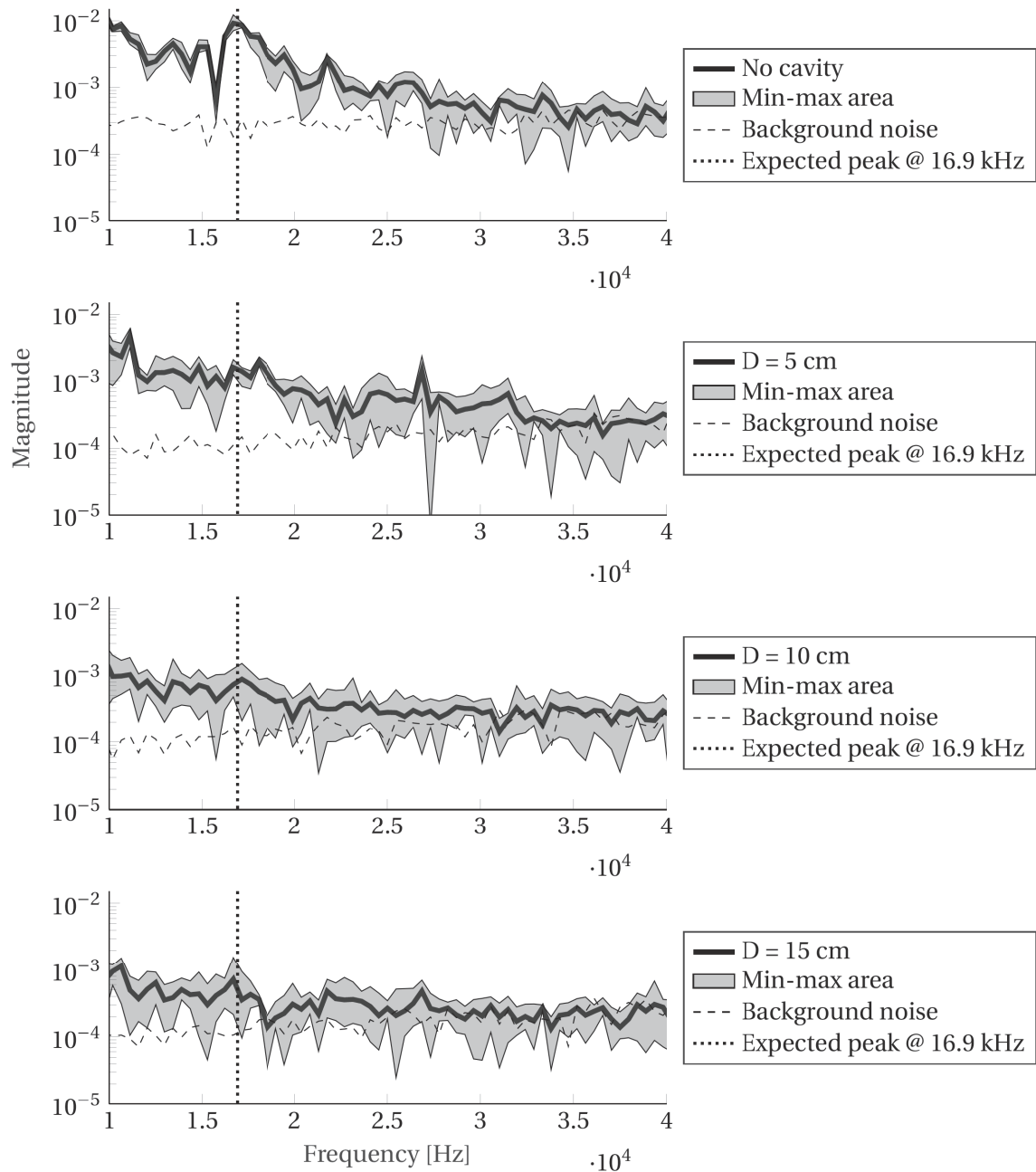


Figure 5.5: Varying support cavity

The samples with 10 cm and 15 cm diameter cavities in the support have a very low impact signal compared to the background noise. From 20 kHz the background noise is at comparable level as the impact vibrations.

5. Discussion

The results do not come close to the expectations. It seems like something went wrong executing this experiment. Only two settings are changed between experiments: The impactor positioning and the particle velocity sensor placement. The impact force data is stored during the experiment. To verify if the impact was correct, the maximum force is compared with last correct experiment. The average maximum force for each situation is shown in table 5.3.

A significantly lowered impact force is seen. This might have caused the flat response. The PWM and powering time settings are not changed in the impactor device. The positioning of

Table 5.3: Average maximum force per situation

Sample name	Average maximum force
No cavity	131 N
D = 5 cm	98 N
D = 10 cm	44 N
D = 15 cm	47 N

the impactor device above the samples must have been off. To verify this the experiment should be repeated with the impactor positioned precisely like in the other experiments.

Although unlikely the positioning of the particle velocity sensor might also have played a role. The influences of the placement are not investigated in this report, but in order to know for sure if the small changes in positioning influence the measurements this should be done.

6. Conclusion

The positioning of the particle velocity and/or impactor in the experimental setup is sensitive. With this dataset nothing about cavities in the supporting material can be concluded. This experiment should be repeated with the impactor placed at the correct distance in order to get a more substantiated conclusion. The positioning of the particle velocity sensor and influences of the impactor force are interesting for follow-up experiments.

5.4 Varying cavity concrete

1. Motivation

In the failure process described in section 3.1 concrete starts missing at certain points. In this experiment this missing concrete (cavity in the concrete) is tested. Experiment 5.2 tested the thickness of the whole sample. This experiment focuses on local reduced thickness. Artificial cavities are made in the samples. It is assumed these local cavities are filled with air.

2. Experiment design

Three experiments are carried out using the 8 cm thick sample. The impact is still in the middle and the cavities are not filled with sand. The following samples are created with a drill hammer (see figure 5.6):

1. Circular cavity, diameter 5 cm, depth 1 cm. Due to the inaccuracy of the hammer drill the actual cavity depth is 12 mm to 14 mm.
2. Circular cavity, diameter 10 cm, depth 1 cm. Due to the inaccuracy of the hammer drill the actual cavity depth is 12 mm to 14 mm.
3. Circular cavity, diameter 10 cm, depth 2 cm. Due to the inaccuracy of the hammer drill the actual cavity depth is 24 mm to 26 mm.

3. Hypothesis and calculations

Three effects are expected during this experiment (see section 3.2.3):

- An extra thickness frequency corresponding to the depth of the cavity.
- Depending on the size and depth of the cavity a shifted or no peak at all for the original sample thickness.
- Because the cavity surface is rough, the reflection angles will not be perfect. This probably results in a lower amplitude of the thickness frequencies, due to the reduced reflections.

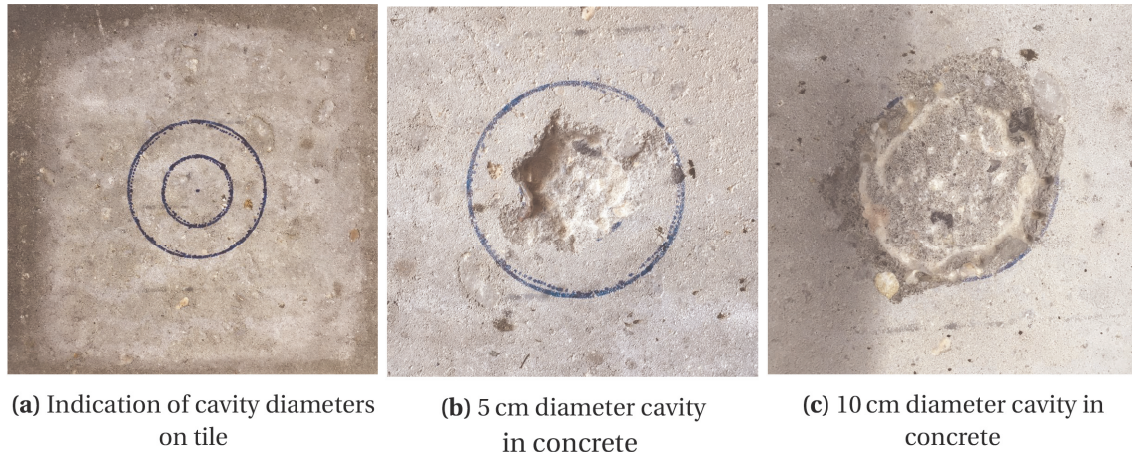


Figure 5.6: Artificial created cavities in the concrete tile

The size-depth ratio of the cavities is calculated to determine which scenario of section 3.2.3 is applicable.

- No cavity: Scenario (a) applies. There will be one peak for the thickness.
- $\varnothing 50 \times 13$ mm: $\frac{d}{T} = \frac{50}{70} \approx 0.7 > \frac{1}{3}$. The size of the flaw is larger than $\frac{1}{3}$ of the depth. Scenario (c) applies. The thickness frequency of the 8 cm thick tile will lower both in frequency and amplitude and a peak corresponding to depth of the flaw is expected.
- $\varnothing 100 \times 13$ mm: $\frac{d}{T} = \frac{100}{70} \approx 1.4 < 1.5$. The size of the flaw is smaller than 1.5 times the depth of the flaw. Scenario (c) applies again. The thickness frequency of the 8 cm thick tile will lower both in frequency and amplitude and a peak corresponding to depth of the flaw is expected.
- $\varnothing 100 \times 25$ mm: $\frac{d}{T} = \frac{100}{58} \approx 1.7 > 1.5$. The size of the flaw is larger than 1.5 times the depth of the flaw. Scenario (d) applies. No frequency peak of the undamaged part is expected. The low frequency peak f_{flex} is out scope of this research and not expected in the analysed frequency range.

The expected thickness frequencies for both the cavity and undamaged concrete are calculated using equation 5.4 and the new calculated P-wave speed.

- Without cavity: Concrete thickness is 83 mm, so the frequency peak is expected at 16.9 kHz
- 1 cm deep cavity: Actual thickness of concrete under impact point is approximately 70 mm, so the peak is expected at 20 kHz.
- 2 cm deep cavity: Actual thickness of concrete under impact point is approximately 58 mm, so the peak is expected at 24.2 kHz.

4. Results

The results of the four (three with cavity and one without for reference) situations are shown in figure 5.7. The result of the sample without cavity is of the experiment redone and not copied from previous experiments.

The declining frequency content for frequencies lower than 10 kHz is ignored. The sample without cavity shows again a global peak for the thickness frequency. The 5x1 cm cavity shows a remarkable frequency peak at approximately 29 kHz. The same peak - however smaller in amplitude - is present by the other samples with cavity.

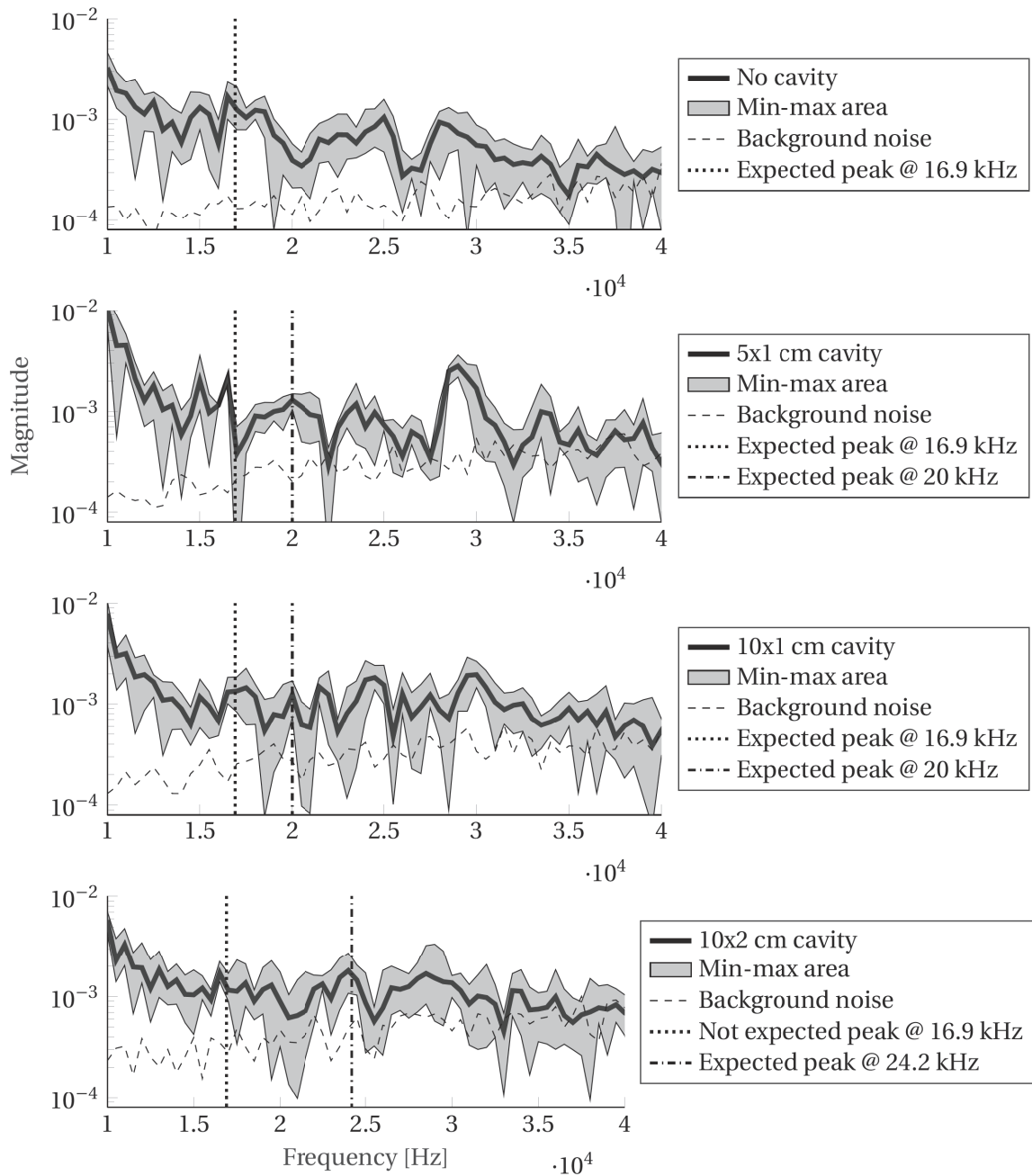


Figure 5.7: Results samples with varying cavity in concrete

Overall a lot of local peaks are present in the signal. All samples with cavity lack a clear peak at the thickness frequency.

In order to see what changes every time the cavity is enlarged, the differences between the results are displayed in figure 5.8.

No outstanding peaks are present in the differences between situations.

5. Discussion

No global peaks are found at the expected positions for the samples with cavities. The origin of all the other present peaks is unknown.

The sample with the 10x2 cm cavity still shows a small peak at 16.9 kHz. This can mean two things: Either the peak is not only the thickness frequency, or the theory is not fully correct and this peak is still a residue of the thickness frequency.

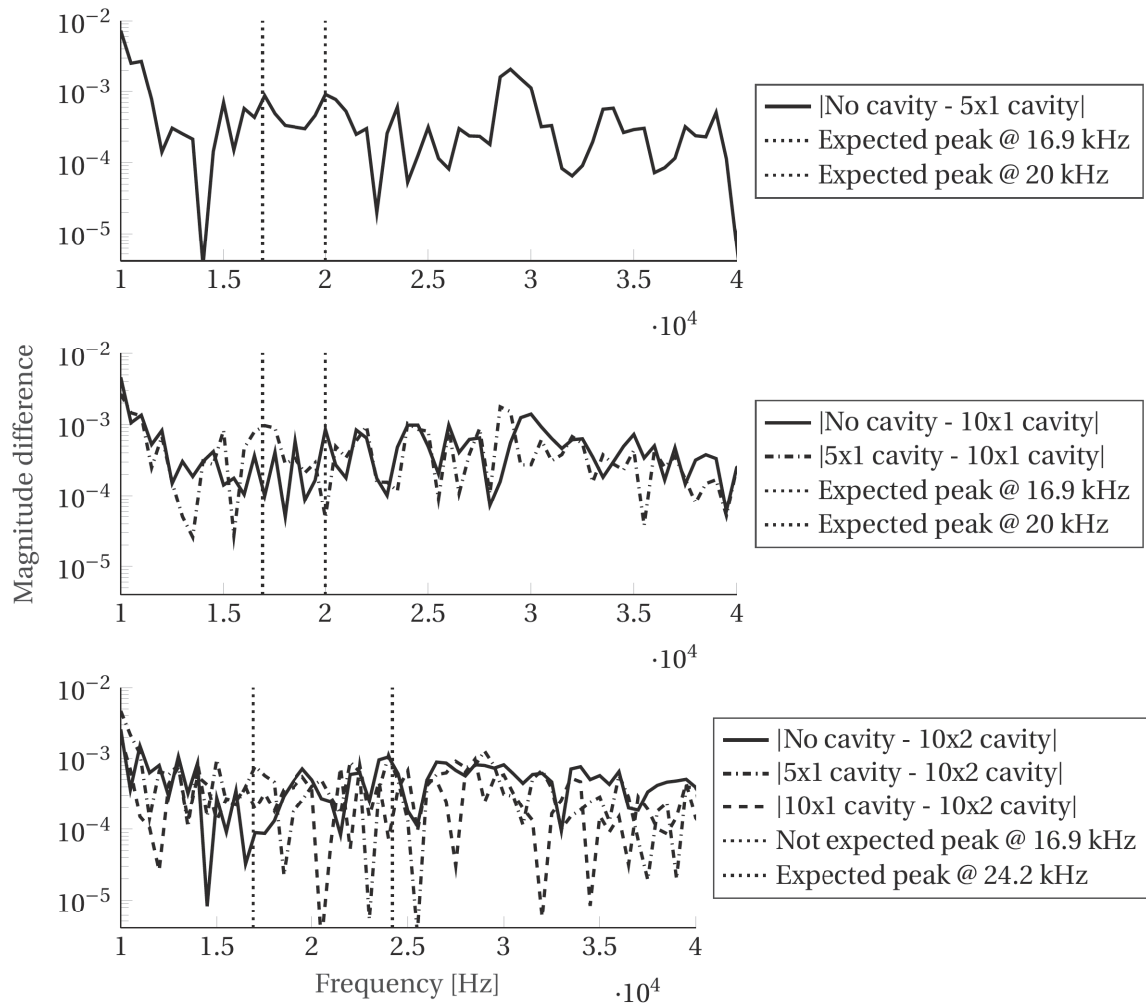


Figure 5.8: Differences between situations

6. Conclusion

Cavities in concrete cannot be detected accurately. Some frequency peaks seem to correspond to expected values, however the amplitude compared to other unknown peaks is too little to use them for unknown samples. A correct contact time of the impactor can help.

5.5 Varying background noise

1. Motivation

When a particle velocity sensor is used correctly in combination with the very-near-field effect, less background noise influence is expected (see section 3.4). An experiment is carried out in order to quantify this advantage. Various levels of background noise are tested to determine at which level the particle velocity sensors stands out from a microphone.

2. Experiment design

For this experiment again the 8 cm thick tile is used. A waveform generator (Agilent 33220A) is used to generate Gaussian (white) noise. The noise is played on two speakers. White noise is chosen in order to influence all frequencies equally. The speakers are placed as shown in figure 5.9. The distance between the sensors and speakers is 25 cm.

Five levels of background noise are tested: 40 dBA, 50 dBA, 60 dBA, 70 dBA and 80 dBA. The dBA unit is common and corrects for the human ear sensitivity. The normal sound level is around 40 dBA in the lab, and an increase of 10 dB corresponds to a tenfold increase of power. This is measured with a sound level meter (type Lutron SL-4001, see figure 5.10) at the same position as the particle velocity sensor and microphone.



Figure 5.9: Background noise speaker placement, **Figure 5.10:** Background noise measurement approximately 25 cm from the sensor setup using Lutron SL-4001

For this experiment a different model particle velocity sensor is used: the PU Regular of Microflow is chosen. This model has a microphone and particle velocity sensor at the same place, so measurements can easily be compared.

3. Hypothesis and calculations

It is expected that the microphone measures more background noise compared to the particle velocity sensor. For low levels of background noise this is expected not to be a problem. For higher levels of background noise, the microphone measurements are expected to be useless, since the noise will overrule the surface vibrations.

Due to the very near field conditions it is expected that not all frequencies are measured in the very near field. Frequencies up to 1150 Hz will probably be in the very near field (see section 4.3). The frequencies not measured in this field will not benefit from the background noise reduction due to the very near field.

The amount of noise reduction (compared to a pressure microphone) depends on the distance to the sound source, see figure 5.11. In this figure the difference in Signal-to-Noise Ratio between a microphone and particle velocity sensor in front of vibrating objects (a rigid circular piston and square wooden plate) is shown for various distances. The green line shows the values for 10 mm distance to the source, which is used in this experiment.

As can be seen in figure 5.11, the reduction depends also on the frequency of the signal. Because square tile of 30 cm × 30 cm are used, it is expected the square plate (right figure) gives the most comparable results.

For low frequencies - 750 Hz and lower - the noise reduction is high. No data is presented for the frequencies interesting for the P-wave analysis (10 kHz to 40 kHz), but the very near field noise reduction effect will cease.

Because our measurements cannot directly be linked to decibels, the Signal-to-Noise Ratio (SNR) is calculated for the measurements (see equation 5.5). This value is expressed in decibels because of the large dynamic range, but it is still a ratio.

$$SNR_{dB} = 20 \log_{10} \frac{U_{impact}}{U_{noise}} \quad (5.5)$$

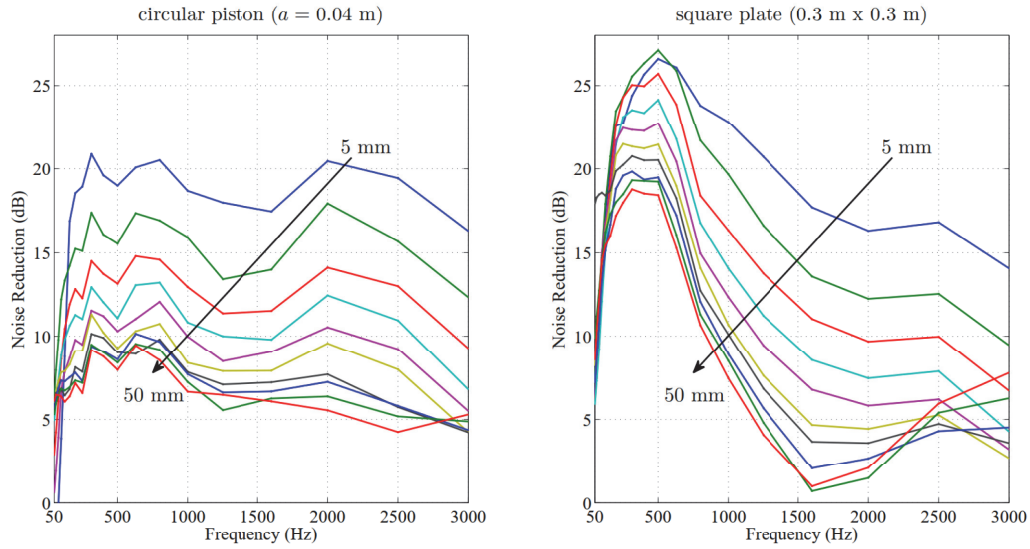


Figure 5.11: Noise reduction in front of a rigid circular piston (left) and square wooden plate (right) for several distances to the source (Comesana et al., 2014)

U is the signal voltage in V. U_{noise} is measured right before the impact, U_{impact} is measured during the impact. The higher the Signal-to-Noise ratio, the better the surface vibrations are received compared to the noise.

4. Results

In figure 5.12 a comparison in SNR between microphone and particle velocity sensor is shown for various levels of background noise. The particle velocity sensor SNR is always lower than the

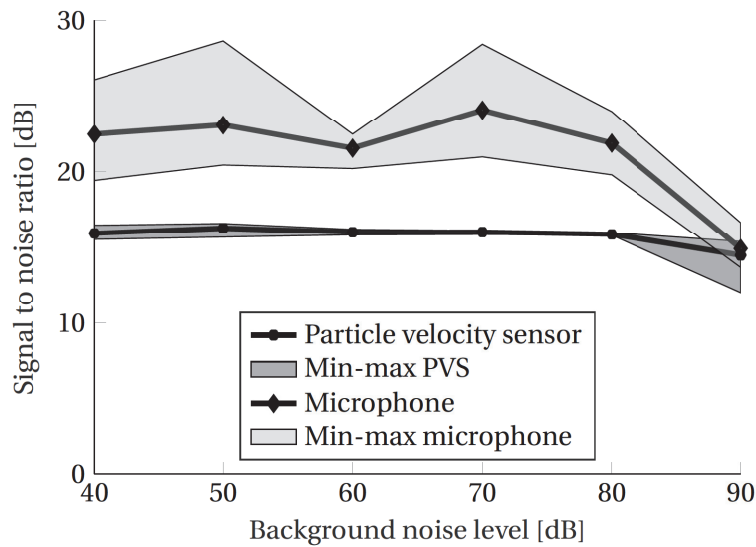


Figure 5.12: Signal noise ratio for various levels of background noise

microphone measurement. The SNR of the particle velocity sensor is more constant and only shows a minor drop at 90 dBA. The microphone measurements show more variance between the measurements and a steep decline at 90 dBA.

In figure 5.13 the microphone is compared to the Particle Velocity Sensor (PVS) for three levels of background noise per frequency.

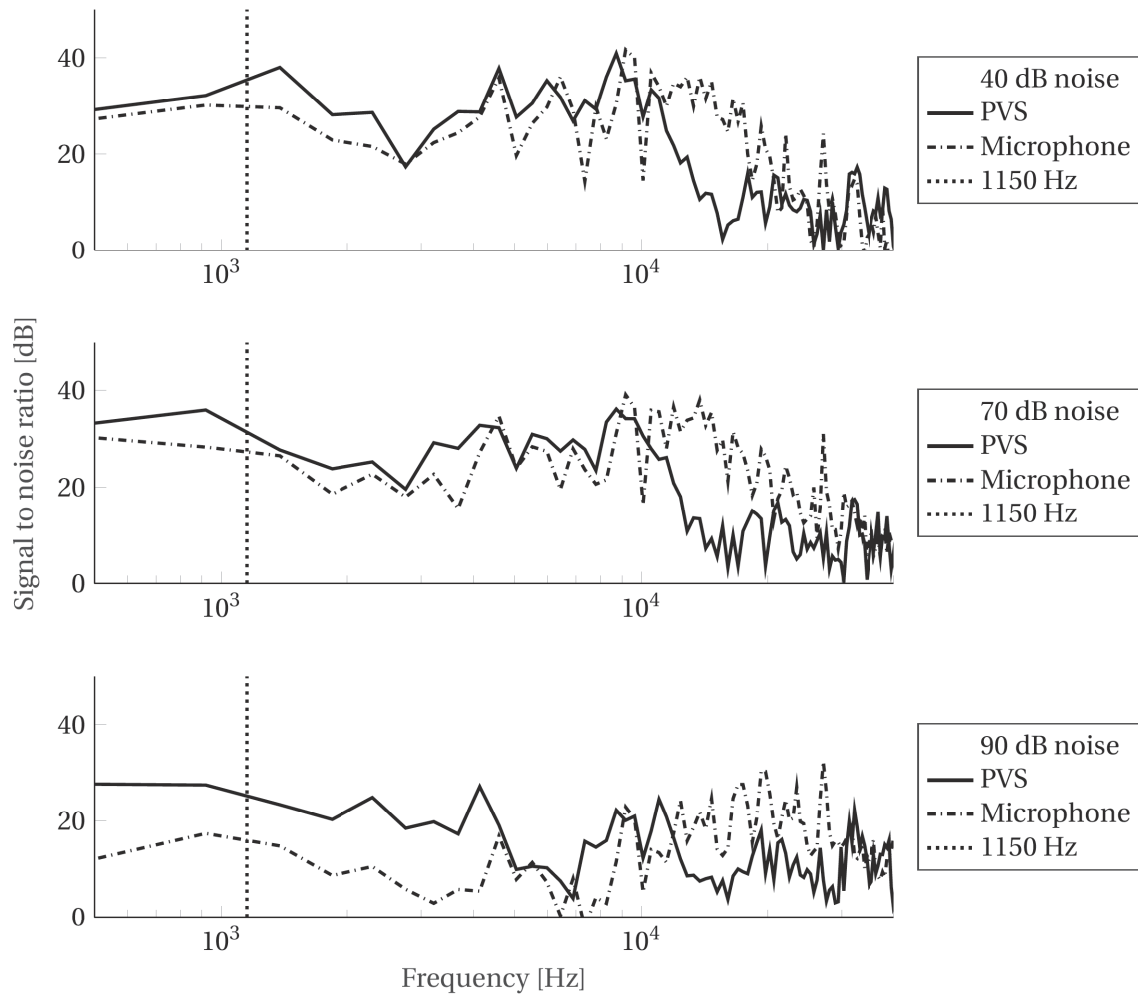


Figure 5.13: Signal noise ratio for various levels of background noise per frequency

Up to approximately 5 kHz the particle velocity sensor shows a higher Signal-to-Noise Ratio than the microphone. Especially for high background noise levels (see 90 dB) the microphone has a low SNR for low frequencies. The PVS still has a decent SNR by 90 dB up to 4 kHz. For higher frequencies (> 10 kHz) the PVS has a poor SNR no matter the background noise level.

5. Discussion

The background noise reduction was not present for high frequencies as expected. Low frequencies can be measured with a particle velocity sensor in presence of background noise. Higher frequencies are better received with a normal microphone, but the influence of background noise is bigger. Especially for low frequent vibrations are overruled with noise by microphone measurements.

The whiteness of the generated noise is debatable. Speakers are normally designed for frequencies up to 20 kHz, so higher frequencies are probably damped. Comparing the particle velocity sensor and microphone for frequencies higher than 20 kHz is therefore impossible without verifying the whiteness first.

6. Conclusion

For low frequencies - up to 4 kHz - the particle velocity sensor has a good Signal-to-Noise Ratio compared to a microphone even for high levels of background noise. For higher frequencies the microphone shows better results. For impact echoes high frequent reflections are important, so a microphone seems like a better option.

5.6 Varying surface humidity

1. Motivation

In practise most measurements will be done in wet environments. Not only can the surface be wet, also the concrete can absorb some water. It is a useful insight to know how this influences condition measurements.

2. Experiment design

Three situations are tested. For all tests the 8 cm thick tile is used.

1. Dry: This sample is used for reference.
2. Wet surface: The surface of this sample is sprayed with water just before impact. The tile is not submerged before.
3. Submerged: This sample is submerged in water for 24 h, this way all internal cavities are filled with water instead of air. After the submerging it is placed in the sample support tub and tested. There is no water layer on top of the tile.

3. Hypothesis and calculations

Five effects of the wet surface are expected:

- The wet layer adds a reflection. The impact will still directly vibrate the concrete, but before the vibration is measured, it must pass through the wet layer. The water layer will reflect more than half of the vibration. Therefore the measured signal after the water layer will be lower in amplitude.
- The water layer can add a frequency peak corresponding to its own thickness. The frequency will be out of range of the measurement since the layer is extremely thin.
- The humidity will probably induce some damping. The damping will result in an overall reduced response.
- The impact can generate a wave motion in the water. Because this wave starts before the concrete is impacted, the influences are filtered together with the R-wave.
- The filling of internal cavities with water in the concrete influences the reflections. Water reflects waves only partial, while air reflects waves completely. More of the original P-wave can reach the back of the concrete.

Since the 8 cm thick tile is used, the thickness frequency is still expected at 16.9 kHz for all situations. Water has a reflection coefficient between -0.65 and -0.75 . A coefficient of -0.7 is assumed. Approximately 70 % signal loss is expected if the vibrations must travel through a water layer before surfacing.

If assumed that the submerging in water fills all air cavities in the concrete with water, the vibration signal of the sample thickness improves. An air cavity reflects all waves, so all air cavities the P-wave encounters before reaching the back of the concrete sample do not result in reflections related to the total thickness. A water cavity reflects approximately 70 % of the P-waves, so only 30 % will pass through. If assumed that the wave passes through the same cavity twice before surfacing - and thus being measured - $30\% \cdot 30\% = 9\%$ will contribute to the total thickness frequency of the concrete. The magnitude of frequencies above the thickness frequency will lower slightly due to this.

The amount of air cavities in the concrete is unknown. Therefore, the expected increase of the thickness frequency cannot be calculated.

4. Results

In figure 5.14 the results of this experiment are shown.

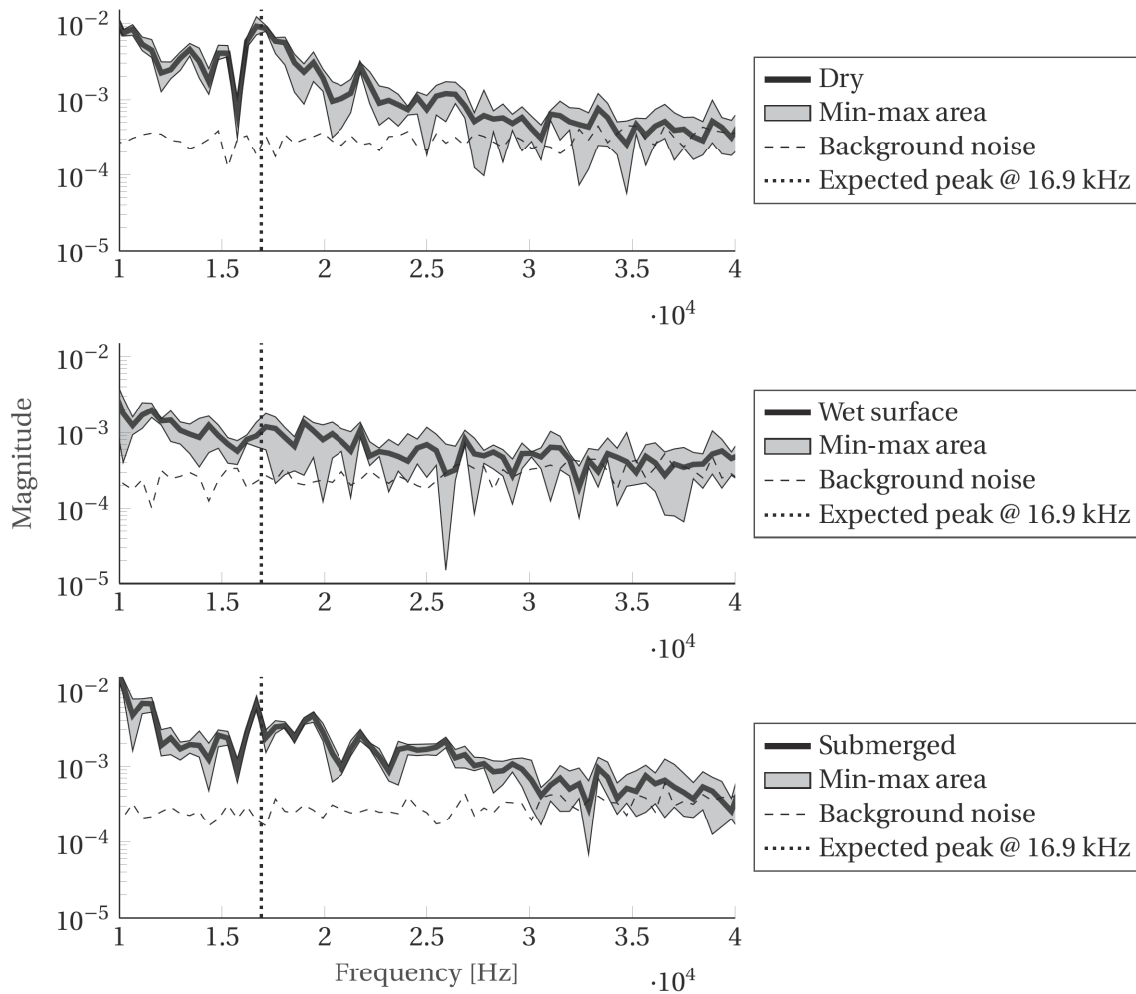


Figure 5.14: Varying surface humidity

The wet surface sample shows a remarkable flat frequency spectrum, especially if compared to the sample which was submerged for one day. The submerged sample shows a global peak at the thickness frequency. The submerged sample shows overall low variance compared to the other situations.

The wet surface sample shows a lower magnitude across the whole frequency spectrum. The difference between noise and impact vibrations is less compared to the submerged and dry samples.

In table 5.4 the average frequency magnitude between 10 kHz and 40 kHz and the thickness frequency magnitude is shown. The background noise is subtracted to minimise influences of the particle velocity placement between the situations. A large decrease in magnitude is seen

Table 5.4: Difference in response between 10 kHz and 40 kHz

Sample name	Average frequency magnitude		Thickness frequency magnitude	
Dry	1.8×10^{-3}	100 %	9.0×10^{-3}	100 %
Wet surface	0.46×10^{-3}	26 %	0.7×10^{-3}	7.5 %
Submerged	1.9×10^{-3}	106 %	6.5×10^{-3}	73 %

for the wet surface sample compared to the dry reference sample. The thickness frequency is not identifiable. The submerged sample shows an overall increased response. The thickness frequency magnitude has lowered compared to the dry sample.

5. Discussion

The expected reduced vibration measurement happened for the sample with wet surface. The expected thickness frequency cannot be recognised anymore.

The overall increased response of the submerged sample was not expected. The reduced thickness frequency magnitude is also opposite of expected. The thickness frequency is still a global peak at the expected frequency.

It is unsure why the magnitude changes are different than expected for the submerged sample. It might be due to slight changes in setup between the two situations. The slightest difference in positioning of the particle velocity sensor as well as the impactor can influence the whole measurement. Influences of the positioning should be investigated in future research.

Also, the frequency range for which the average frequency magnitude is calculated is arbitrary. A cavity in the concrete close to the surface can result in a frequency peak higher than 40 kHz. It is impossible to distinguish exactly between the P-wave and noise.

6. Conclusion

A fully soaked concrete sample - all internal cavities are filled with water - without a water layer on top shows comparable results to a dry sample. A small layer of water on the surface makes impact echoes with the current setup impossible.

6 Conclusion & Recommendations

6.1 Conclusion

To what extent can an acoustic impact echo using a particle velocity sensor assess the condition of a concrete sewer pipe?

It was expected that using a particle velocity sensor for contactless vibrations measurements condition assessment of sewer pipes was possible. Due to less background noise influences the particle velocity sensor should perform better than a microphone. It was tried to answer this question by means of a literature study and by performing experiments. In the experiments it was tried to define the usability of the particle velocity sensor for different measurement conditions. The results of the experiments are used to draw some first conclusions about the use of particle velocity sensors in assessing the condition of concrete sewer pipes.

None of the experiment results showed very clear frequency peaks, therefore assessment was hard or impossible. This is due to the damping of the interesting frequencies by the too long contact time of the impactor. It was still possible to link local peaks to expected thickness frequencies for thicker structures. For thin structures the thickness frequency is not recognisable due to the lower sensitivity for higher frequencies. It is expected thickness frequencies up to 20 kHz can be detected correctly. Due to the damped response assessment of cavities in both the support and concrete itself is impossible for unknown samples.

The promising noise cancellation property of the particle velocity sensor was not of influence in these measurements. The very near field effect is limited to low frequencies which are not of interest in impact echoes.

Although experiments should be repeated with a correct impact time, it can be concluded that the particle velocity sensor can be used in humid sewer pipes. Concrete which is submerged in water for a long period of time - 24 h for experiments - shows an identical vibration response compared to dry concrete. However, a layer of water in the sewer should be avoided as this damps the measured vibrations.

To conclude, the use of a particle velocity sensor for impact echoes is not advised. Experiments indicate that the microphone has an increased sensitivity for higher frequencies and is still usable with background noise. Therefore - although the particle velocity sensor is useable - a microphone is probably a better measurement tool for assessing the condition of concrete sewer pipes contactless than the particle velocity sensor.

6.2 Recommendations

The measurements with the particle velocity sensor were not reliable due to the assumptions about contact time. A different impact device is required to perform impact echoes with a correct impact time. This can be achieved in several ways, an example of this is shown in figure 6.1. The impactor steel ball has little inertia besides its own mass, in this case the contact time assumption for steel balls is justified.

The performed measurements can be compared to a normal impact echo in order to verify the results obtained with the particle velocity sensor. It is recommended to repeat the experiments with both a surface mounted transducer and a particle velocity sensor. Without this comparative measurement it remains uncertain if these experiments are performed correctly. In this way it can be verified whether the results obtained with the particle velocity sensor are reliable compared to other available methods.

At this moment it is not known which force is needed to perform a correct impact echo. It is assumed that higher forces are needed for thicker concrete. A force sensor is already incor-

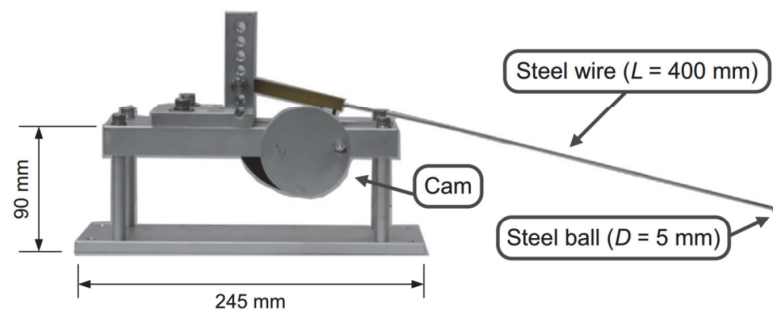


Figure 6.1: Alternative impact device (Kang et al., 2017)

porated in the developed impact device and could therefore be easily used to determine the impact force needed for correct impact echoes. With this new information the impact force of the performed measurements can be verified.

Furthermore, thought can be given to the correlation between impact force data and the rebound value, thus compressive strength. The ratio between the force towards and backwards from the surface is expected to correlate to the rebound number. Therefore, it can be measured with the current setup.

Lastly, the placement of the particle velocity sensor can be examined. In this report the location of the sensor is determined with help of the very near field conditions and a guideline for surface mounted transducers. By testing various positions, the placement can be verified or improved.

A Sand composition

The average result of two sieve analysis is shown in table A.1. Using the visual representation in figure A.1 the three characteristic values D-values can be determined: D10 = 0.25 mm, D50 = 0.52 mm and D90 = 1.4 mm.

Table A.1: Sieve analysis of sand

Sieve size [mm]	Sand in sieve [g]	Cumulative weight [%]	Cumulative weight passing [%]
5.6	0	0	100
4	0	0	100
2	15.5	4.84	95.16
1.4	17	5.30	89.86
1	20.5	6.40	83.46
0.6	65.5	20.44	63.03
0.5	48.5	15.13	47.89
0.3	104	32.45	15.44
0.15	46.5	14.51	0.94
0.125	1	0.31	0.62
Box	2	0.62	0.00
Total	320.5 g	100 %	

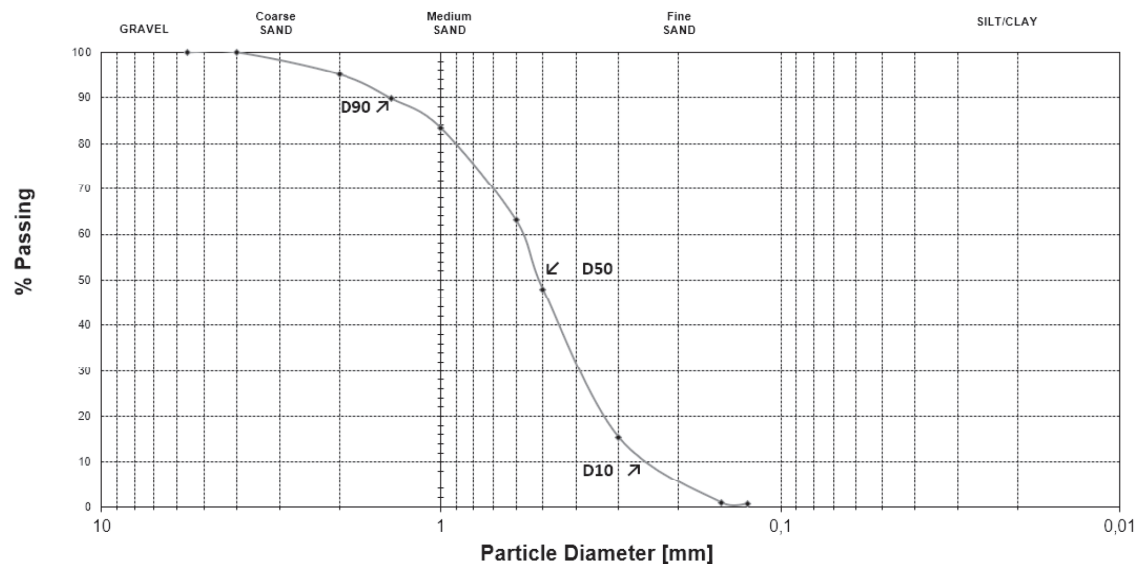


Figure A.1: Sand composition graph

B Impact device wiring details

In this appendix the electrical wiring of the impactor device is shown. The wiring is split in several figures for clarity.

B.1 User I/O

The wiring of the five push buttons is displayed in figure B.1.

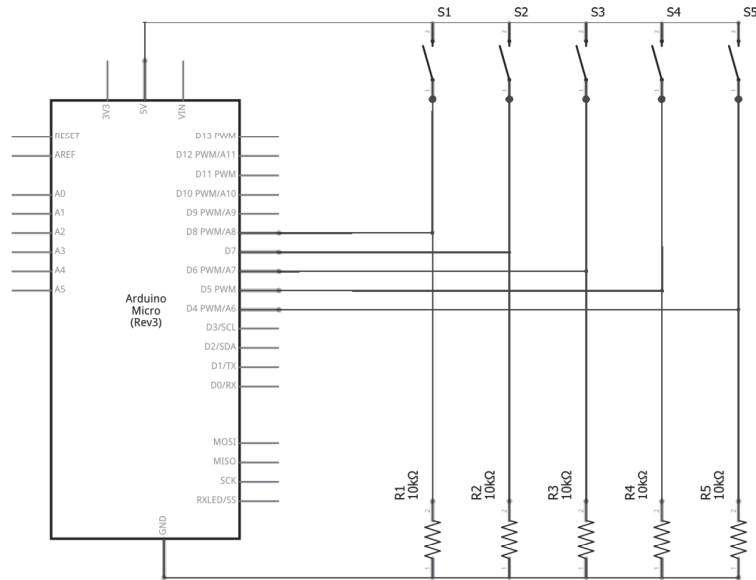


Figure B.1: Button wiring

The user output is displayed on a 16x2 display of Joy-iT (COM-LCD16X2), see figure B.2 for the wiring.

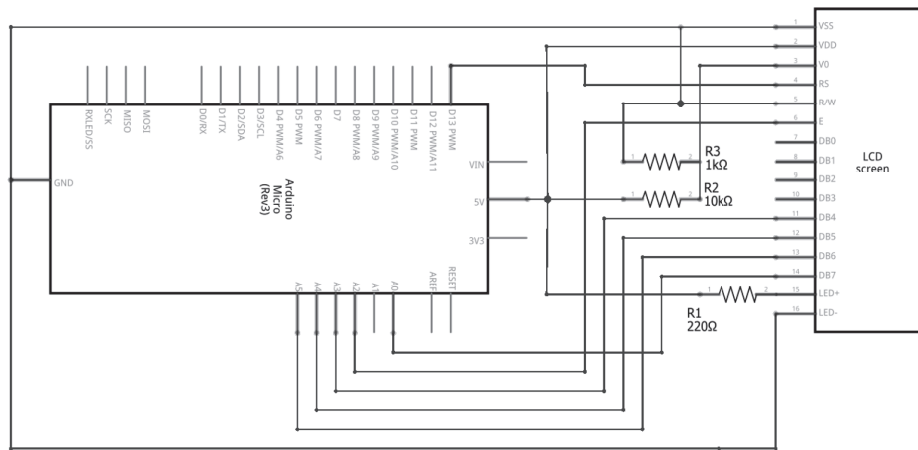


Figure B.2: Display wiring

The I/O module is displayed in figure B.3.



Figure B.3: I/O module

B.2 Solenoid

The solenoid (ITS-LS 5852 12VDC of Red Magnetics) is powered by a high power transistor. A flyback diode avoids the back electromotive force from destroying the Arduino. The transistor is mounted on a heatsink. The solenoid powering module is shown in figure B.5 and wiring in figure B.4.

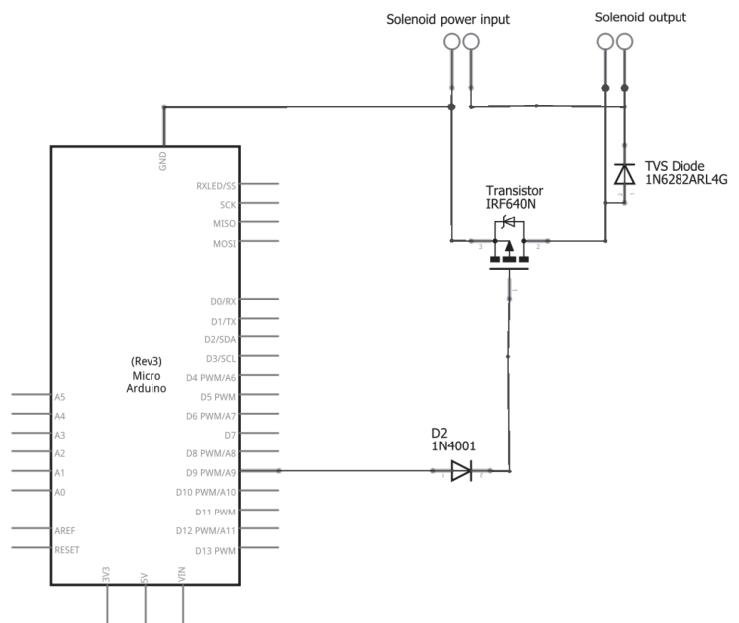


Figure B.4: Solenoid wiring

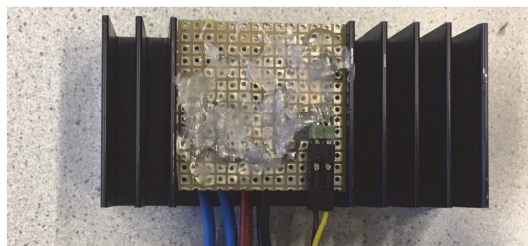


Figure B.5: Solenoid powering module

B.3 Sensors and micro-controller

In figure B.6 the wiring of sensors is shown. The main board with all connectors is shown in figure B.7. The external sensors are shown in figure B.8.

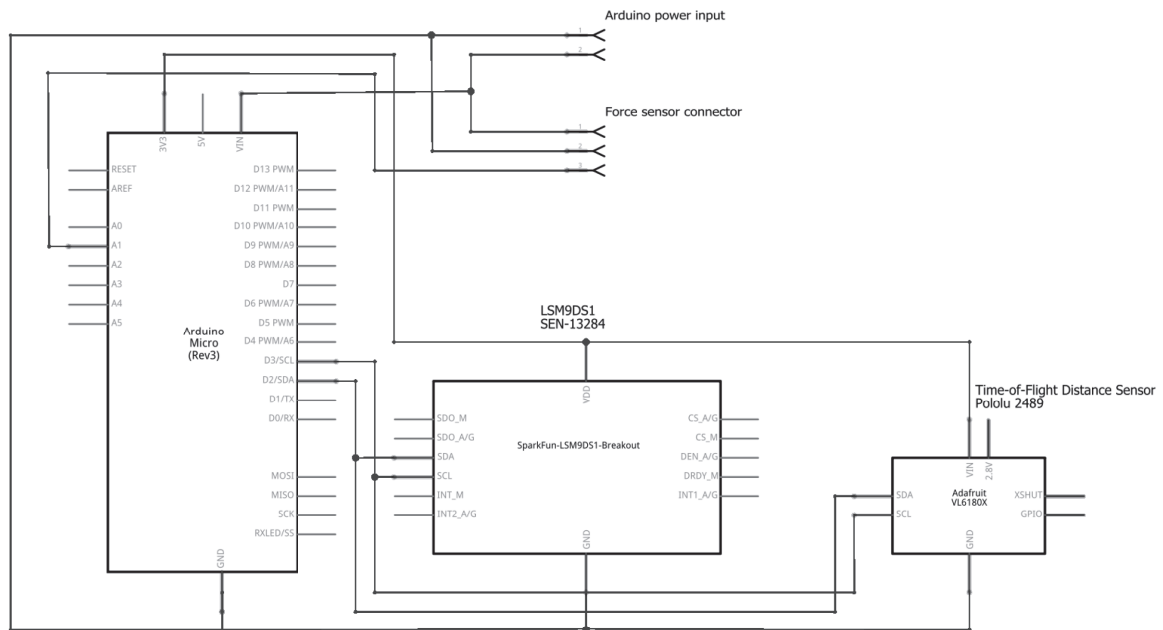


Figure B.6: Sensors wiring

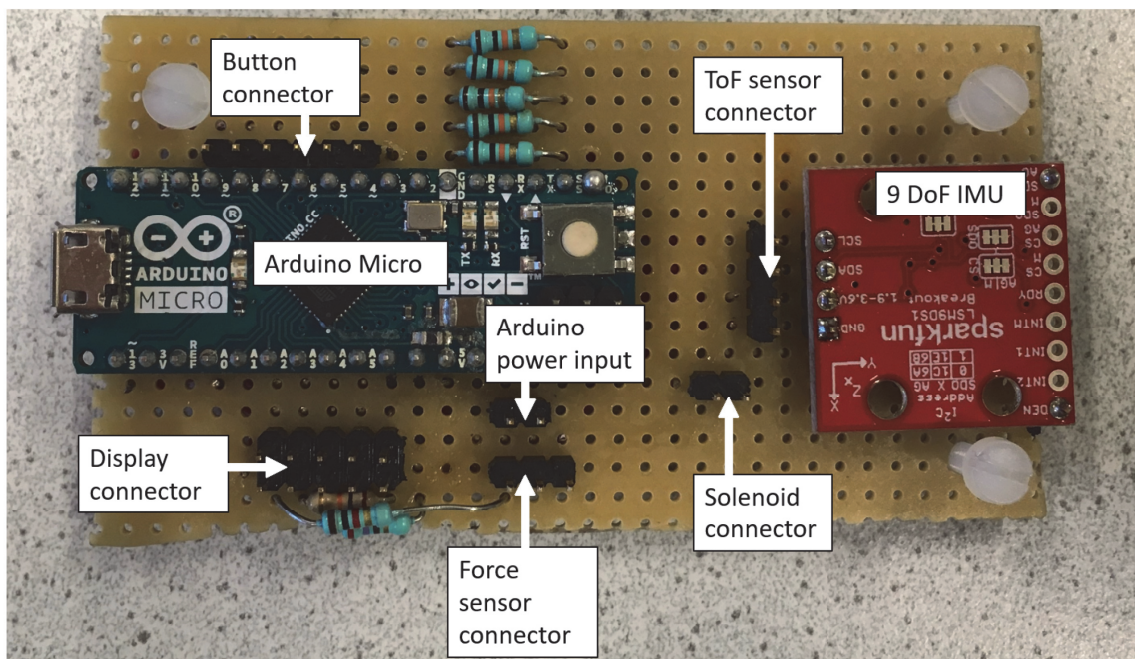


Figure B.7: Main board with connectors and 9-DoF sensor



(a) Force sensor amplifier

(b) Time-of-Flight distance sensor

Figure B.8: External sensors

C Impact device Arduino code

```

// Display driver and wiring
#include <LiquidCrystal.h>
const int rs = 13, en = A2, d4 = A3, d5 = A4, d6 = A5, d7 = A0; // Dispaly wiring
LiquidCrystal lcd(rs, en, d4, d5, d6, d7);

// Pinout solenoid & buttons
const int solenoid = 9, button_1 = 8, button_2 = 7, button_3 = 6, button_4 = 5,
      button_5 = 4;

// Button variables
bool st_b1 = 0, pr_b1 = 0, b_impact = 0; // Impact button
bool st_b2 = 0, pr_b2 = 0, b_tdown = 0; // Time down button
bool st_b3 = 0, pr_b3 = 0, b_tup = 0; // Time up button
bool st_b4 = 0, pr_b4 = 0, b_pwmdown = 0; // PWM down button
bool st_b5 = 0, pr_b5 = 0, b_pwmup = 0; // PWM up button

// Setting variables
int impact_pwm = 255; // 0-255
int impact_time = 22; // [ms]

void setup() {
  // Setup display and show version
  lcd.begin(16, 2);
  lcd.print("IMPACTOR_v0.5");

  // Ready for normal operation
  delay(500);
  lcd.clear();
  lcd.print("PWM:_____");
  lcd.print(impact_pwm);
  lcd.setCursor(0, 1);
  lcd.print("Time_(ms):_");
  lcd.print(impact_time);

  // I/O defined
  pinMode(solenoid, OUTPUT);
  pinMode(button_1, INPUT);
  pinMode(button_2, INPUT);
  pinMode(button_3, INPUT);
  pinMode(button_4, INPUT);
  pinMode(button_5, INPUT);
}

void loop() {

  // ////////////////////////////////////
  // BUTTONS
  // ////////////////////////////////////
  st_b1 = digitalRead(button_1);
  st_b2 = digitalRead(button_2);
  st_b3 = digitalRead(button_3);
  st_b4 = digitalRead(button_4);
  st_b5 = digitalRead(button_5);

  // Impact
  if (st_b1 == 1 && pr_b1 == 0) {
    b_impact = 1;
    pr_b1 = 1;
  }
}

```

```

else if (st_b1 == 0) {
    pr_b1 = 0;
}
// Time down
if (st_b2 == 1 && pr_b2 == 0) {
    b_tdown = 1;
    pr_b2 = 1;
}
else if (st_b2 == 0) {
    pr_b2 = 0;
}
// Time up
if (st_b3 == 1 && pr_b3 == 0) {
    b_tup = 1;
    pr_b3 = 1;
}
else if (st_b3 == 0) {
    pr_b3 = 0;
}
// PWM down
if (st_b4 == 1 && pr_b4 == 0) {
    b_pwmdown = 1;
    pr_b4 = 1;
}
else if (st_b4 == 0) {
    pr_b4 = 0;
}
// PWM up
if (st_b5 == 1 && pr_b5 == 0) {
    b_pwmup = 1;
    pr_b5 = 1;
}
else if (st_b5 == 0) {
    pr_b5 = 0;
}

// //////////////////////////////////////
// SETTINGS
// //////////////////////////////////////
// PWM
if (b_pwmup == 1) {
    b_pwmup = 0;
    impact_pwm = impact_pwm + 1;
    if (impact_pwm > 255) {
        impact_pwm = 255;
    }
}
if (b_pwmdown == 1) {
    b_pwmdown = 0;
    impact_pwm = impact_pwm - 1;
    if (impact_pwm < 0) {
        impact_pwm = 0;
    }
}
// Time
if (b_tup == 1) {
    b_tup = 0;
    impact_time = impact_time + 1;
    if (impact_time > 200) { // Max 200 ms powering solenoid
        impact_time = 200;
    }
}
if (b_tdown == 1) {

```

```
b_tdown = 0;
impact_time = impact_time - 1;
if (impact_time < 0) {
    impact_time = 0;
}
}

// Show settings
lcd.setCursor(11,0);
lcd.print("  ");
lcd.setCursor(11,0);
lcd.print(impact_pwm);
lcd.setCursor(11, 1);
lcd.print("  ");
lcd.setCursor(11,1);
lcd.print(impact_time);
delay(20);

//////////
// IMPACT
//////////
if (b_impact == 1) {
    b_impact = 0;
    analogWrite(solenoid, impact_pwm);
    delay(impact_time);
    analogWrite(solenoid, 0);
    delay(500); // Avoid unintended impacts
}
}
```

Listing C.1: Arduino code for impactor device

Bibliography

- de Bree, H., V. Svetovoy, R. Raangs and R. Visser (2004), The very near field theory, simulations and measurements of sound pressure and particle velocity in the very near field, in *Eleventh Congress on Sound and Vibration at Petersburg, 2004*.
- Bungey, J. H., S. G. Millard and M. G. Grantham (2006), *Testing of Concrete in Structures*, Taylor & Francis, 4 edition, ISBN 9780415263016.
- Carino, N. J. (2001), The Impact-Echo Method: An Overview, *Structures Congress & Exposition*, doi:10.1061/40558(2001)15.
- Carino, N. J. (2015), Impact echo: the fundamentals, in *International Symposium Non-Destructive Testing in Civil Engineering (NDT-CE), Berlin, Germany*.
- Carino, N. J., M. Sansalone and N. N. Hsu (1986), Flaw detection in concrete by frequency spectrum analysis of impact-echo waveforms, *International advances in nondestructive testing*, vol. 12, pp. 117–146.
- Colla, C. and R. Lausch (2003), Influence of source frequency on impact-echo data quality for testing concrete structures, vol. 36, no.4, pp. 203 – 213, ISSN 0963-8695, doi:[https://doi.org/10.1016/S0963-8695\(02\)00062-2](https://doi.org/10.1016/S0963-8695(02)00062-2), structural Faults and Repair.
<http://www.sciencedirect.com/science/article/pii/S0963869502000622>
- Comesana, D. F., F. Yang and E. Tijs (2014), Influence of background noise on non-contact vibration measurements using particle velocity sensors, *Proceedings to Internoise*.
- Davies, J., B. Clarke, J. Whiter and R. Cunningham (2001), Factors influencing the structural deterioration and collapse of rigid sewer pipes, vol. 3, no.1, pp. 73 – 89, ISSN 1462-0758, doi:[https://doi.org/10.1016/S1462-0758\(01\)00017-6](https://doi.org/10.1016/S1462-0758(01)00017-6).
<http://www.sciencedirect.com/science/article/pii/S1462075801000176>
- de Bree, H. and W. Druyvesteyn (2005), A particle velocity sensor to measure the sound from a structure in the presence of background noise, in *Forum Acousticum*.
- Gibson, A. and J. S. Popovics (2005), Lamb wave basis for impact-echo method analysis, vol. 131, no.4, pp. 438–443.
- Helal, J., M. Sofi and P. Mendis (2015), Non-destructive testing of concrete: A review of methods, vol. 14, no.1, pp. 97–105.
- Kang, J. M., S. Song, D. Park and C. Choi (2017), Detection of cavities around concrete sewage pipelines using impact-echo method, *Tunnelling and Underground Space Technology*, vol. 65, pp. 1 – 11, ISSN 0886-7798, doi:<https://doi.org/10.1016/j.tust.2017.02.002>.
<http://www.sciencedirect.com/science/article/pii/S0886779816302395>
- Raangs, R. (2005), *Exploring the use of the Microflown*, Ron Raangs.
- Tekscan (2018), FlexiForce A201 Sensor, [Online; accessed 3 Dec, 2018].
<https://www.tekscan.com/products-solutions/force-sensors/a201>
- Prof. dr. Z. Su, A.S.Z. El-Said, H. N. M. (2017), Technology Innovation for Sewer Condition Assessment - Long-distance Information-system (TISCALI).
- Zhu, J. and J. S. Popovics (2007), Imaging Concrete Structures Using Air-Coupled Impact-Echo, vol. 133, no.6, pp. 628–640, doi:10.1061/(ASCE)0733-9399(2007)133:6(628).
<https://ascelibrary.org/doi/abs/10.1061/%28ASCE%290733-9399%282007%29133%3A6%28628%29>